University of Crete

Studying the role of a genetically linked pair of plant NLR Immunity receptors

Master thesis

Mentzelopoulou Andriani
Supervisor: Assist. Prof. Sarris Panagiotis
November 1st, 2019

Contents

1. Introduction

1.1 Plant immunity system

Plant damage and cessation of their growth and development due to biotic stresses, result in yield losses for crops every year, essential for food, fibre and biofuel production (Zhang, et al., 2019). In their natural environment, plants co-exist with microbial communities and therefore, during their co-evolution, the former have developed specific, induced and highly regulated immunity mechanisms in order to become resistant to several diseases (Brader et al., 2014; Zhang, et al., 2019). This co-evolutionary cycle is known by the term "Red Queen dynamics" (Han, 2018). Plant defense mechanisms can be divided into two categories: the preliminary, basal defense called pathogen-associated molecular pattern (PAMP) triggered immunity (PTI) (Monaghan & Zipfel, 2012) and the secondary defense, effector-triggered immunity (ETI) (Eitas & Dangl, 2010). More specifically, as suggested by Jones J. and Dangl J. in 2006, the plant immunity system can be depicted as a "zig-zag" scheme (Fig. 1) (Jones & Dangl, 2006). This model will be analyzed in detail further down, in the next sections.

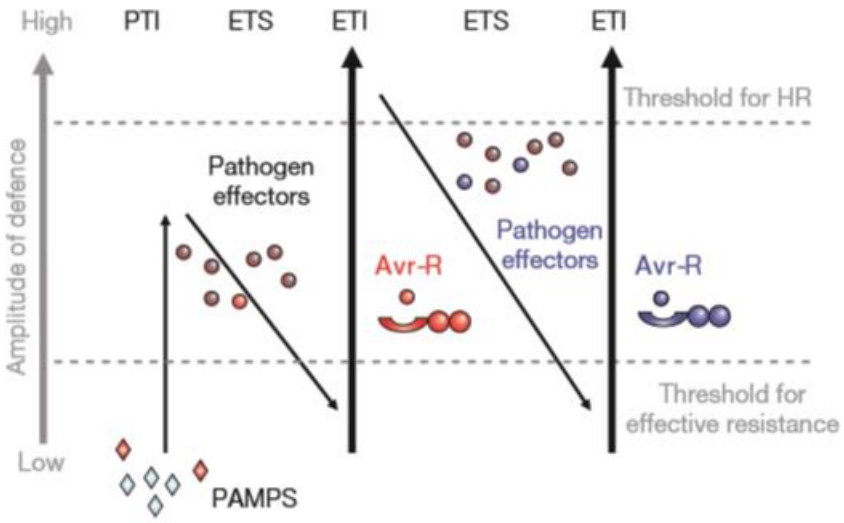

***Figure 1**. "Zig-zag" model of the plant innate immunity system (Jones J. & Dangl J., 2006).*

1.2 PAMP triggered immunity (PTI)

PAMP triggered immunity constitutes the first phase of the zig-zag model, therefore the first layer of the plant defense mechanisms (Jones & Dangl, 2006). More specifically, plant cells perceive infection through receptors found on their plasma membrane, called pattern recognition receptors (PRRs). PRRs recognize pathogen or microbe associated molecular patterns (PAMPs or MAMPs), which are conserved molecular characteristics of the pathogens and are common in entire groups of microbes, such as chitin, peptidoglycans or flagellin (Boller & Felix, 2009). In addition, PRRs also recognize the so-called damage associated molecular patterns (DAMPs), which originate from the host plant cells, that were subject to infection (cell wall fragments, cutin monomers, peptides) (Boller & Felix, 2009; Jones & Dangl, 2006; Nicaise et al., 2009). PRRs are divided mostly into two categories: i) receptor like kinases (RLKs) and ii) receptor like proteins (RLPs). RLKs contain a leucine-rich repeat (LRR) extracellular domain, a trans-

membrane domain and an intracellular kinase domain. RLPs' only difference from RLKs is that they contain a shorter intracellular domain without a specific function (Maekawa et al., 2011; Wang, et al., 2007). Intracellular kinase domains contribute to the signal transduction for the initiation of downstream defense responses (Erwig, et al., 2017; Yeh, et al., 2016). More specifically, mitogen-activated protein kinases (MAPKs) are activated through phosphorylation and are involved in the activation of multiple defence responses such as the biosynthesis of plant stress or defense hormones (salicilic acid, jasmonic acid or ethylene), the production of reactive oxygen species (ROS), stomatal closure and cell wall thickening (Meng & Zhang, 2013). Hence, further colonization of the pathogen is restricted (Jones & Dangl, 2006).

1.3 Effector triggered immunity (ETI)

During the second phase of the "zig-zag" model, pathogens in turn employ multiple virulence effectors to overcome the PTI defense responses and successfully establish infection. This results in effector triggered susceptibility (ETS) (Jones & Dangl, 2006). During the third phase, virulence effectors are recognized by specific plant cell receptors called NLRs (containing nucleotide binding site and leucine rich repeats), leading to effector triggered immunity (ETI) (Takken & Goverse, 2012). ETI is an amplified PTI response and leads to disease resistance and usually to hypersensitive response (HR), a highly controlled phenomenon, which involves programmed cell death (PCD), so that the pathogens do not spread further than the infection site (Dodds & Rathjen, 2010; Greenberg, 1996; Jones & Dangl, 2006). Other NLR-effector recognition responses are Ca^{2+} influx, production of ROS, activation of the MAPK path, endomembrane trafficking and transcriptional alteration (Cui et al., 2015).

NLR receptors derive from the resistance genes (R genes). NLRs have a conserved nucleotide binding domain (NB), also known as NB-ARC (nucleotide binding adaptor shared by Apaf1, certain R genes and CED4) and a C terminal leucine rich repeat domain (LRR) (Takken & Goverse, 2012). The NB-ARC domain participates in the control of nucleotide binding and hydrolysis (Takken et al., 2006). Additionally, this domain interacts with the LRR domain and the NLR remains at an inactive, autoinhibited state when the effector protein is absent (Moffett et al., 2002). Moreover, other domains have been identified at the N terminal; the toll and interleukin-1 receptor domain (TIR), the coiled coil domain (CC) and the RPW8-like type domain. Depending on these N-terminal domains NLRs are grouped into three subgroups; the TIR-NLRs (TNLs), the CC-NLRs (CNLs) and the RPW8-NLRs (RNLs). These variable N-terminal domains often play a role in signaling (Cesari, 2017).

According to Flor H., in 1971, "for each gene that conditions resistance in the host (R gene) there is a corresponding gene that conditions pathogenicity in the parasite (AVR gene)", thus, a singleton NLR interacts with a pathogen effector. In this model, the NLR receptor plays the role of the "sensor" and the "helper (signal inducer)" at the same time, meaning that it detects the virulence effector and, also, helps in sending the signal to the downstream defense responses, respectively (Adachi et al., 2019; Flor, 1971). A well-studied singleton NLR belongs to the MILDEW LOCUS A (MLA) protein family and provides resistance to powdery mildew fungi (Maekawa, et al., 2019).

On the contrary, in most cases, NLRs form dimers or complexes or appear to work in pairs. It is speculated that, during the evolutionary process, singleton NLRs duplicated and specialized into "sensors" and

"helpers", where a "sensor" NLR and a "helper" NLR collaborate for the recognition of the effectors (Adachi et al., 2019). The NLR is activated when ATP bounds to the NB-ARC domain and under the presence of an effector the NLR is found in a more stable active state (Bonardi et al., 2012; Chiang & Coaker, 2015). Additionally, interaction between the N terminal of NLRs is required for their dimerization or oligomerization and, thus, their proper function. It has also been shown that truncated TIR or CC domains overexpressed can lead to HR in plants (Maekawa et al., 2011). The activation of the NLR receptors is depicted in detail in figure 2. A studied pair of NLR receptors, which are also genetically linked, are RRS1 and RPS4, originally found in *Arabidopsis thaliana*, providing the plant with resistance to *R. solanacearum, P. syringae, C. higginsianum* pathogens (Gassmann et al., 1999).

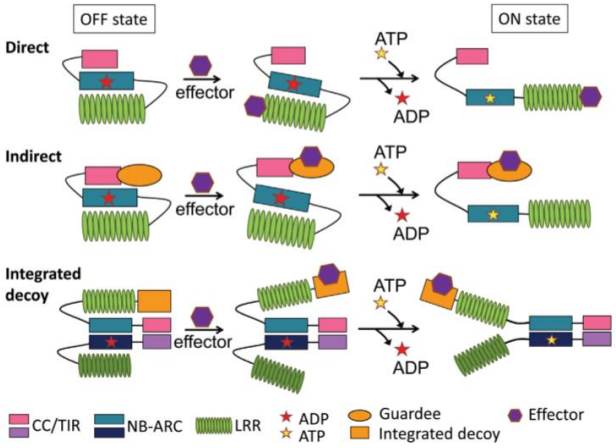

Figure 2. NLR activation process *(Chiang & Coaker, 2015)*.

Apart from the direct recognition of the effector proteins by the singleton NLR receptors, indirect recognition is most commonly identified. More specifically, three models have been described so far, the guardee model, the decoy model and the integrated decoy model. In the guardee model, the NLR receptor recognizes a, modified by the effector, host protein, called a guardee. In the decoy model, the NLR receptor, usually the "sensor" NLR receptor, has modifications that mimic a target of the effector. Lastly, as far as the integrated decoy model is concerned, the NLR receptor contains an integrated domain (ID) that constitutes a target of the effector (Fig. 2, 3) (Cesari, 2017; Sarris, et al., 2015). Integrated domains in NLRs play a very important role in the detection of the effector protein and it is speculated that they have evolved by integration of effector targets in the NLR host genes (Baggs et al., 2017). The NLR pair described above, RRS1 and RPS4, has been shown to be following the integrated decoy model, where RRS1 contains at its C terminal a WRKY domain. This WRKY domain works as an integrated domain and it was shown to detect and interact with two specific virulence effectors, AvrRps4 and PopP2 (Sarris, et al., 2015).

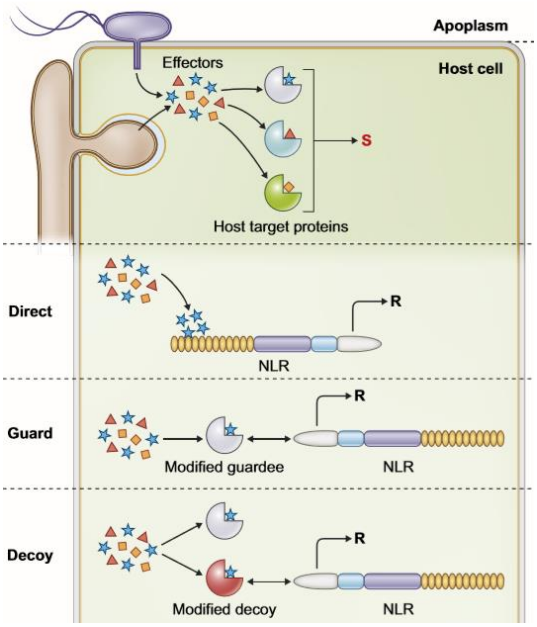

Figure 3. Direct and indirect recognition of effector proteins by NLR receptors, identified models (Cesari, 2017).

1.4 *Bn*RPR1 & *Bn*RPR2

The aim of this master thesis was to study the role of a genetically linked pair of NLR receptors from the *Brassica napus* plant, termed Resistant Pair Receptors 1 and 2 (*Bn*RPR1 and *Bn*RPR2). *Bn*RPR1 contains an NB-ARC domain, an LRR domain and a TIR domain and thus it belongs to the TIR-NLR subgroup. *Bn*RPR2 is also a TNL. As it is shown in figure 5 below, *Bn*RPR1 and *Bn*RPR2 demonstrate a head to head orientation.

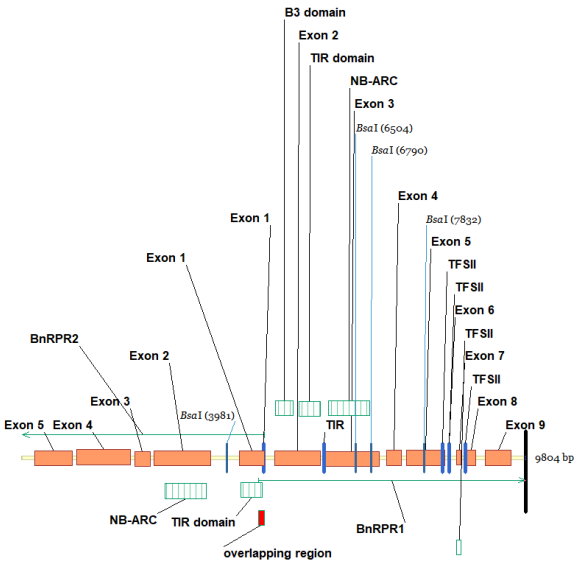

Figure 4. *Bn*RPR1 and *Bn*RPR2 genes map.

More specifically, *Bn*RPR1 contains two important domains that play the role of integrated domains. The N-terminal of the *Bn*RPR1 gene shares great similarity with the B3 DNA binding domain. This domain includes five classes: [1] auxin response factor (ARF), [2] abscisic acid-insensitive3 (ABI3), [3] high level expression of sugar inducible (HSI), [4] related to ABI3/VP1 (RAV) and [5] reproductive meristem (REM) (Romanel et al., 2009). The C terminal of the *Bn*RPR1 gene is similar to the TFIIS domain, which encodes for a transcript elongation factor that induces efficient transcription by the RNA polymerase II (Grasser, et al., 2009).

Moreover*, Bn*RPR1 and *Bn*RPR2 have an overlapping region of 126bp. This common region coincides with the 5' untranslated region (5' UTR) of *Bn*RPR1.

It has already been shown by Amartolou (thesis, 2019) that when *Bn*RPR1 and *Bn*RPR2 genes are co - expressed in *Nicotiana benthamiana* or *Nicotiana tabacum* leaves through agroinfiltration, a hypersensitive response (HR) is triggered in the absence of any virulence effectors, after 48 hours. On the contrary, when BnRPR1 or BnRPR2 were overexpressed each one alone, HR was not triggered. During this study, different protein tags were used and it was verified that the HR response is not caused due to the presence of a specific tag. Moreover, confocal microscopy observations were conducted in order to examine the subcellular localization of the expressed proteins. It was shown that *Bn*RPR1 is localized in the nucleus, whereas *Bn*RPR2 is localized in specific spots inside the nucleus that it is speculated to be the nucleoli.

The purpose of this present master thesis is to study the role of the integrated domains of *Bn*RPR1, the role of the overlapping region and lastly the putative interaction of these *Bn*RPR1 with two effectors from Turnip Mosaic Virus. In more detail, it is important, at first, to study the role of the two integrated domains of *Bn*RPR1, the B3 and the TFSII domain, in order to examine which exact domain is essential for the triggering of HR. For this purpose, truncated *Bn*RPR1 genes are engineered, missing the B3 domain or the TFSII domain or both. Each truncated NLR is studied for the triggering of HR, when overexpressed alone or along with *Bn*RPR2, in plant leaves. Additionally, each truncated *Bn*RPR1 gene is observed under the Confocal microscope, in order to examine any changes in their subcellular localization. Furthermore, following the same procedure, the role of the overlapping region is examined. Lastly, the *Bn*RPR1 NLR receptor is analyzed for its interaction with specific virulence effectors from the Turnip Mosaic virus by carrying out yeast 2 hybrid assays.

2. Materials and methods

2.1 Polymerase chain reaction (PCR)

The polymerase chain reaction (PCR) is a technique for DNA amplification and it is used to generate an ample supply of specific DNA segments. The enzyme used is Phusion® High-Fidelity New England Biolabs, NEB). The reaction is set up according to the to the user's manual (table 1) while the denaturation temperature of the primers is calculated each time through a Tm calculator program from NEB (https://tmcalculator.neb.com/#!/main).

***Table 1**. PCR protocol.*

Steps	Temperature	Time
Initial denaturation	98°C	30sec
25-35 cycles	98°C	5-10sec
	45-72°C	10-30sec
	72°C	15-30sec/kb
Final extension	72°C	5-10min
Hold	4°C	

2.2 DNA extraction from agarose gels

PCR products were extracted from agarose gel with the use of "NucleoSpin® Gel and PCR Clean-up kit" (Macherey-Nagel) according to the user's manual.

2.3 Ligation

The DNA ligation protocol is commonly used in molecular cloning projects to physically join a DNA vector to a DNA segment of interest. Through this method, an extra-chromosomal circular DNA is generated, which can replicate autonomously within certain microbial hosts. The reaction is set up in a microcentrifuge tube on ice using a 1:3 vector to insert molar ratio for the indicated DNA sizes. Molar ratios are calculated using NEBioCalculator (https://nebiocalculator.neb.com/#!/ligation). T4 DNA ligase (NEB) is added last and the microcentrifuge tube is incubated at room temperature for two hours.

2.4 Golden Gate

This is a cloning technique, through which a DNA template is inserted in a cloning vector. The restriction enzyme used is BsaI, a type IIS restriction enzyme. Type IIS enzymes generally bind to DNA as monomers and recognize asymmetric DNA sequences. They cleave outside of this sequence, within one to two turns of the DNA, creating overhangs (New England Biolabs Inc., 2019). Since these overhangs are not part of the recognition sequence, they can be customized to direct assembly of DNA fragments. When designed correctly, the recognition sites do not appear in the final construct, allowing for precise, scarless cloning. The reagents used and the protocol are presented in tables 2 and 3 respectively.

Table 2. Golden gate. Reagents used and their concentrations.

Stock	Volume (µl)	Final concentration
10x BSA buffer	2	1x
10x T4 ligase buffer	2	1x
vector	x	
insert	y	
Enzyme BsaI 20u/µl	1	20 u/µl
Enzyme T4 ligase	1	
ddH_2O	up to 20µl	

x, y: The quantity of the insert in ng is known. The volume required from the cloning vector and the insert is calculated each time so as to have $1*10^{10}$ number of copies in the final solution.

Table 3. Golden Gate protocol.

Temperature	Time
37°C	3min
16°C	4min
37°C	10min (x34 cycles)
80°C	5min
12°C	∞

2.5 *E. coli* transformation using heat shock

Competent *Escherichia coli* cells (DH10b or stellar cells) are mixed with the plasmid (ligation product) under sterile conditions, left on ice for 30min and incubated for 90 sec at 42°C. 900 µl of LB is added in each transformant and the tube is left for recovery at 37°C for one and a half hours with continuous shaking *E. coli* cells are harvested by centrifugation and spread on petri plates containing the appropriate antibiotic for 16 hours at 37°C. Liquid cultures are prepared from each colony formed on the plate for further treatment.

2.6 Plasmid isolation using alkaline lysis protocol

An amount of the overnight grown liquid culture is centrifuged at 11.000xg for 30 seconds. The pellet is resuspended sequentially in three different solutions (table 5) and the tubes are centrifuged at 12.600xg for 5 minutes. Pure ethanol 100% is added to the supernatant and the tubes are centrifuged at 12.600xg for 10-20 minutes. The resulting pellet is washed with 70% (v/v) ethanol and the tubes are centrifuged at 12.600xg for 5 minutes. After air-drying the whole amount of ethanol from the tubes, the resulting pellet is dissolved in ddH_2O.

Table 4. Composition of the solutions used during the plasmid isolation process.

solution I	solution II	solution III
500mM glucose 10ml	NaOH 12µl	5M potassium acetate 60ml
500mM EDTA pH 8.0 2ml	SDS 15 µl	Glacial acetate 11.5ml
1M Tris pH 8.0 2.5ml	ddH_2O 273 µl	ddH_2O 28.5 ml
ddH_2O 85.5 ml		
Sterilization and store at 4°C	Store at RT	Store at 4°C

2.7 RNase A treatment

RNase A is added to the plasmid isolated with the alkaline lysis method to a final concentration of 100µg/ml and the sample is incubated at 37°C for 40 minutes.

2.8 Restriction enzyme digestion

This protocol is carried out in order to check the accuracy of the plasmids generated. The protocol is presented in table 5. The results are checked through agarose gel electrophoresis.

Table 5. Restriction enzyme digestion protocol.

Stock	Volume (µl)	Final concentration
Buffer (enzyme activity 100%) 10x	2	1x
Restriction enzyme(s) 10 u/µl	1	1 u/µl
RNase A 10 µg/ml	0.2	1 µg/ml
Template DNA	2-5	
ddH_2O	Up to 20µl	

Incubation at 37°C for two hours.

2.9 DNA purification (phenol-chloroform protocol)

This protocol is used for the purification of nucleic acids from contaminants. The sample is washed with phenol-TEMS, chloroform – isoamyl alcohol 24:1 and CH_3COONa/pure ethanol respectively. More specifically, after the addition of phenol-TEMS the sample is centrifuged at 13.000xg for 5 minutes and the chloroform – isoamyl alcohol 24:1 is added to the aqueous phase. The second wash with CH_3COONa/pure ethanol is performed respectively. The sample rests at -80°C for 15 minutes and is then centrifuged at 12.600xg for 20 minutes. The resulting pellet is treated with ethanol 70%. After the removal of the whole amount of ethanol, the pellet is dissolved in ddH_2O.

2.10 *Agrobacteria* transformation using cold shock

Competent *Agrobacteria tumefaciens* cells (strain C58C1) are mixed with the plasmid under sterile conditions, flash frozen inliquid nitrogen, and incubated for 30 minutes at 37°C. 900 µl of LB is added in each transformant and the tube is left for recovery at 28°C for three hours with continuous shaking. *Agrobacteria* cells are harvested by centrifugation and grown on petri plates containing the appropriate antibiotic for 48 hours at 28°C. Liquid cultures are prepared from each colony formed on the plate for further treatment.

2.11 Agroinfiltration

Liquid cultures of *Agrobacteria* cells grown overnight at 28°C are centrifuged at 210 x g for 10 minutes. After a double volume of 10mM $MgCl_2$ is added to the pellet formed, the sample is centrifuged again at 210 x g for 10 minutes. This step is performed two times. The resulting pellet is dissolved in MES (10mM/$MgCl_2$, 10mM MES). The optical density (600nm) of each sample () is measured using a spectrophotometer. The final samples are prepared so that each one has OD of 0.4. The *Agrobacteria* cells are infiltrated in *Nicotiana benthamiana* or *Nicotiana tabacum* leaves and the results are monitored.

2.12 Confocal microscopy

Nicotiana benthamiana agroinfiltrated leaves are cut in small sections, placed on a drop of water on top of a slide and covered with a coverslip. YFP is excited at 514 nm and mCherry and chlorophyll at 561 nm. The emission is recorded at 530-560 nm for the YFP tag, at 660-700 nm for the chlorophyll and at 600-640 nm for the mCherry tag. Gain is set at 100.

2.13 Yeast 2 Hybrid (Y2H)

This is an *in vivo* technique that allows the detection of protein-protein interactions using living yeast cells as a model organism. This method is based on mating a set of baits versus a set of prays expressed in *Saccharomyces cerevisiae* cells (Brückner et al., 2009). More specifically, a yeast pre-culture is grown overnight at 28°C in YPDA (Yeast Peptone Dextrose Adenine) media. For each transformant 10^8 cells are needed, therefore the yeast culture should have an OD=0.8. This is an indication that the yeast cells are harvested during their exponential growth phase.

The yeast culture is centrifuged at 280g for 4 minutes. The pellet formed is dissolved in an equal volume of ddH_2O and after another centrifugation the pellet is dissolved in 0.1M LiAc. To the resulting yeast pellet, after a last centrifuge at 11.000g for 1 minute, the following solutions are added in order: PEG 50%, ddH_2O, 1μg from each plasmid (bait or pray) and LiAc solution 1M. The transformants are incubated at 30°C for 25 minutes and then at 42°C for 25 minutes. Yeast transformed cells are harvested by centrifugation and are grown on petri plates lacking leucine and tryptophan, at 28°C for 2 or 3 days. The transformants are screened for protein interactions. The protocol is carried out under sterile conditions.

3. Results

3.1 Studying the role of *BnRPR1* and *BnRPR2* in the absence of tags

It has already been proven that when *BnRPR1* along with *BnRPR2* are overexpressed in *Nicotiana benthamiana* or *Nicotiana tabacum* leaves through agroinfiltration, HR is triggered after 48 or 72 hours. On the contrary, HR is not detected when *Bn*RPR1 and *Bn*RPR2 are overexpressed alone, respectively. The two NLR receptor genes were expressed carrying different tags (Amartolou, 2019 thesis). It is stated, though, in bibliography that tags tend to make aggregations. Therefore, a different folding of the tagged protein may affect its function (Costantini et al., 2012). Thus, it must be examined, at first, if the hypersensitive response is provoked due to the presence of tags.

For this purpose, *Bn*RPR1 and *Bn*RPR2 were constructed without tags. In order to eliminate the already existing BsaI cut sites of the genes and because this genomic locus was long, it was separated in different fragments. Therefore, *Bn*RPR1 was separated in four fragments and *Bn*RPR2 in two fragments. In detail, the two last fragments of each gene were amplified via PCR using specific primers where each reverse primer contained a STOP codon. These PCR products were provided by Mermigka Glykeria.

The amplified fragments were then inserted in the T-tailed pBluescript Golden Gate compatible vector (PBLSKGG), via TA cloning. The ligation products were pBLSKGG:*Bn*RPR1-4STOP and pBLSKGG:*Bn*RPR2-2STOP. The plasmids were used for the transformation of *E. coli* competent cells (strains DH10b or Stellar). The mini prep products were digested with restriction enzymes in order to verify that the ligation has been correctly performed. pBLSKGG:*Bn*RPR1-4STOP was digested with BamHI/HindIII and the expected sizes were 2931, 1231, 522bp. pBLSKGG:*Bn*RPR2-2STOP was digested with BamHI/HindIII and the expected sizes were 2931, 2368, 954, 456bp. The results of the restriction enzyme digestions are shown in figure 6. The plasmid maps designed using the Vector NTI program can be found at the supplementary data section (supplementary data figure A).

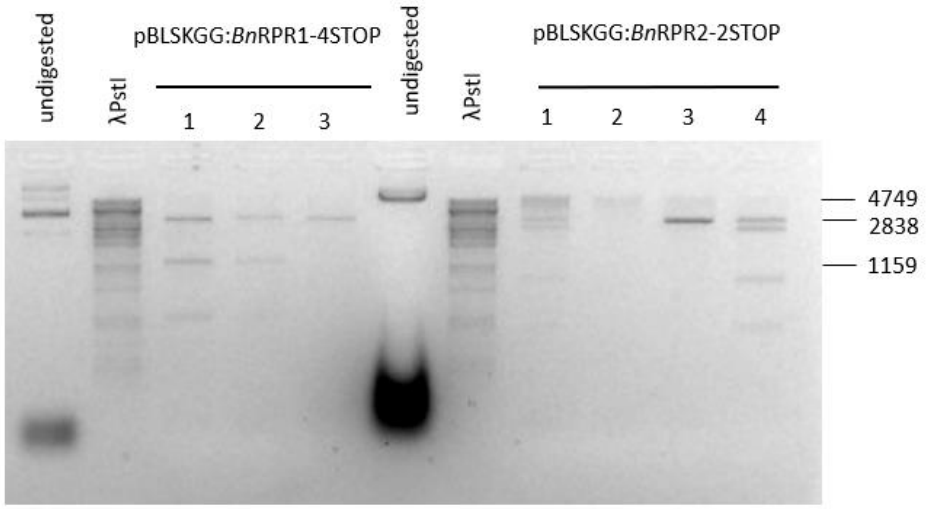

Figure 5. *Restriction enzyme digestion results of pBLSKGG:BnRPR1-4STOP* and *pBLSKGG:BnRPR2-2STOP.* Restriction enzymes used: BamHI/HindIII. Expected sizes: 2931, 1231, 522 bp and 2931, 2368, 954, 456 bp respectively. Samples 3, 5 and 6 were not taken into consideration.

The constructs in pBluescript (pBLSKGG:BnRPR1-1STOP & *pBLSKGG:BnRPR2-2STOP*), were then inserted in the pICH86988 vector along with the rest of the fragments, using the Golden Gate protocol. The Golden Gate products were *pICH86988:BnRPR1STOP* & *pICH86988:BnRPR2STOP*. These constructs were also checked via restriction enzyme digestion (figures 7, 8). The plasmid maps designed using the Vector NTI program can be found at the supplementary data section (supplementary data figure B).

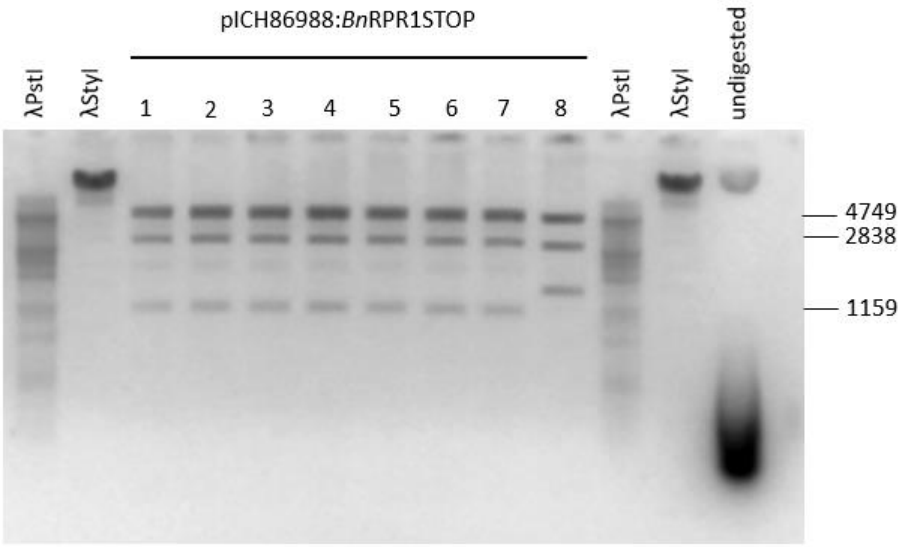

Figure 6. Restriction enzyme digestion results of pICH86988*:Bn*RPR1STOP. Restriction enzymes used: BamHI/ApaII. Expected sizes: 5077, 4458, 2677, 1110 bp. Sample number 8 was not taken into consideration.

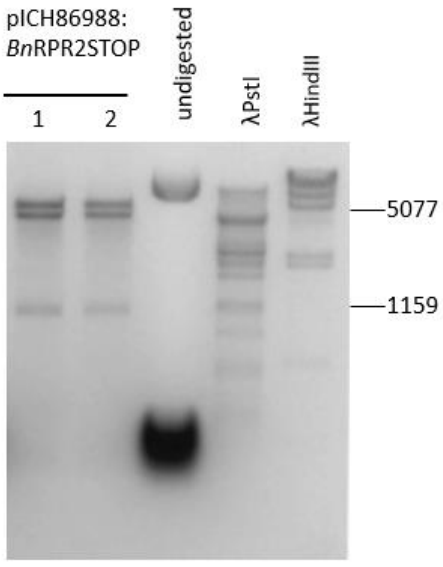

Figure 7. Restriction enzyme digestion results of pICH86988*:Bn*RPR2STOP. Restriction enzymes used: BamHI/PstI. Expected sizes: 6654, 5073, 1096, 132 bp.

The transformed *A. tumefaciens* cells with the constructs engineered were used for agroinfiltration assays. The tissue used for this experiment was *Nicotiana benthamiana* or *Nicotiana tabacum* leaves. The agroinfiltration assay was performed in patches on the leaf surface. More specifically, *Bn*RPR1:YFP and *Bn*RPR2:mCherry were overexpressed as a positive HR control. *Bn*RPR1STOP and *Bn*RPR2STOP were overexpressed together and each one alone in different patches. This experiment was repeated three times.

The agroinfiltration results indicate that the tags do not alter the triggering of the hypersensitive response at the area of the injection. The overexpression of the two NLR genes without tags leads to HR. *Bn*RPR1STOP or *Bn*RPR2STOP alone do not result in HR. We can conclude that the presence of fluorescence tags does not affect the cause of HR. Therefore, we can move forward and study the role of this genetically linked pair of NLR receptors (figure 9).

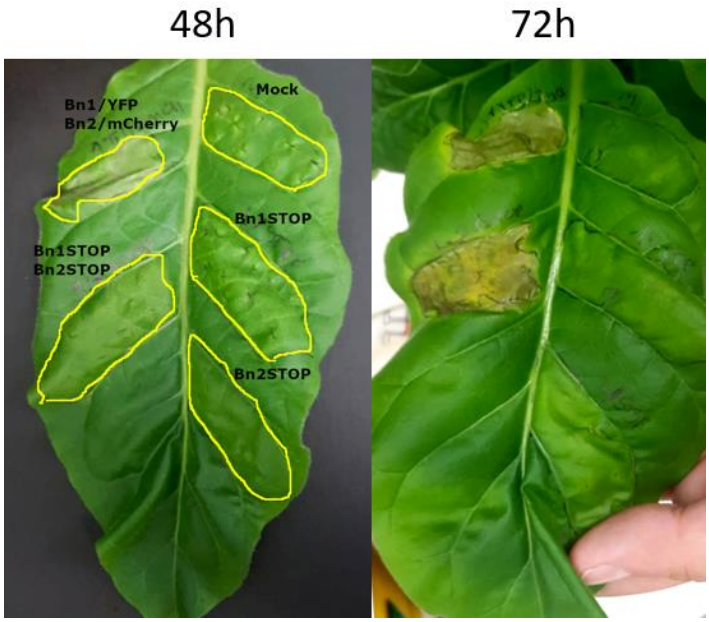

Figure 8. Agroinfiltration results. *Bn*RPR1 co-expressed with *Bn*RPR2 triggers HR with or without the presence of tags, respectively, after 72 hours. *Bn*RPR1STOP or *Bn*RPR2STOP expressed alone do not trigger HR. *N. tabacum* leaves were used for this agroinfiltration assay and the experiment was repeated three times.

3.2 Role of the integrated domains of *Bn*RPR1

In this master thesis, the role of the two genes is being studied, at first, by examining the role of the two integrated domains of *BnRPR1*, B3 and TFSII. The B3 domain is found at the N terminal of the *BnRPR1* gene and thus at the first fragment whereas the TFSII domain is found at the C terminal and at the fourth fragment of the gene (figure 10).

Figure 9. The four fragments of BnRPR1 gene and the location of the integrated domains. The B3 domain is found at the N terminal of the gene and at the first fragment whereas the TFSII domain is found at the C terminal and at the fourth fragment.

For this purpose, certain constructs, truncations of *BnRPR1*, were designed and engineered, in order to specify which exact domain of *BnRPR1* (B3 or TFSII or both) is responsible for the triggering of HR in the plant. More specifically, the first fragment of *Bn*RPR1 without the B3 domain and the fourth fragment of *Bn*RPR1 without the TFSII domain were amplified using specific primers. These PCR products were provided by Mermigka Glykeria.

Following the same experimental process as with *Bn*RPR1STOP and *Bn*RPR2STOP, the amplified fragments were inserted in the pBluescript vector. The ligation products were pBLSKGG:*Bn*RPR1-1ΔB3 and pBLSKGG:*Bn*RPR1-4ΔTFSII. In order to validate that the TA cloning has been performed correctly, the plasmids were digested with restriction enzymes. pBLSKGG:*Bn*RPR1-1ΔB3 was digested with BamHI/HindIII and the expected sizes were 2931, 1267 bp. pBLSKGG:*Bn*RPR1-4ΔTFSII was digested with BamHI/HindIII and the expected sizes were 2931, 415 bp. The results of the restriction enzyme digestions are shown in (figures 11, 12). The plasmid maps designed using the Vector NTI program can be found at the supplementary data section (supplementary data figure A).

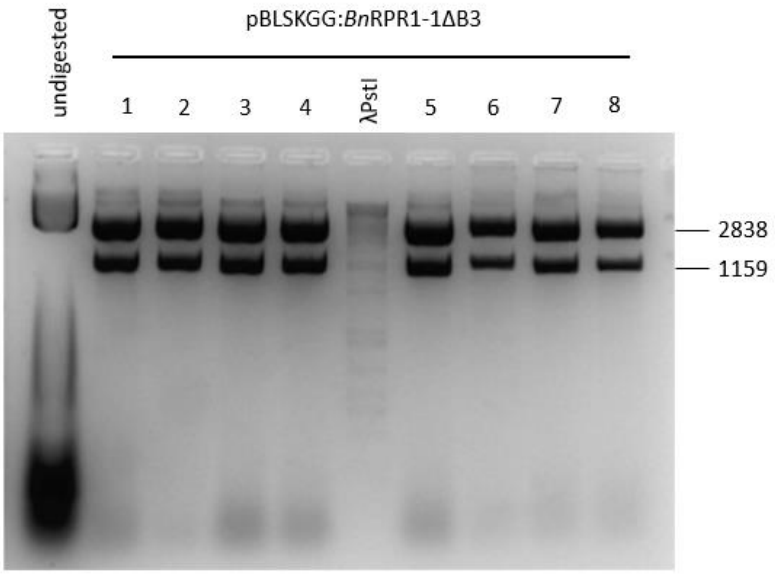

Figure 10. Restriction enzyme digestion results of pBLSKGG:*Bn*RPR1-1ΔB3. Restriction enzymes used: BamHI/HindIII. Expected sizes: 2931, 1267 bp.

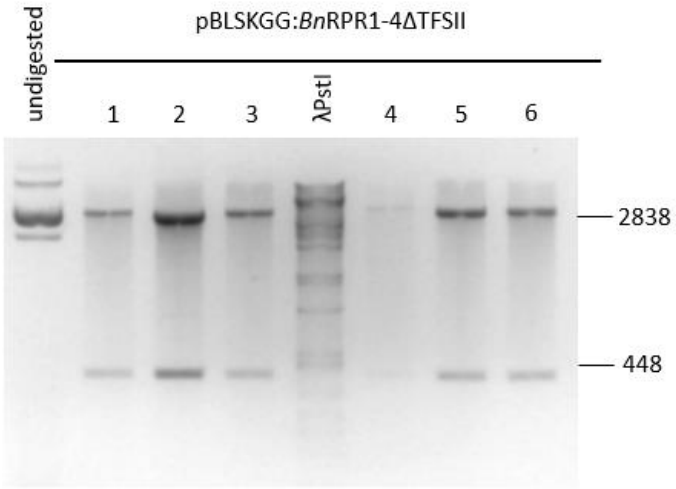

Figure 11. Restriction enzyme digestion results of pBLSKGG:*Bn*RPR1-1ΔTFSII. Restriction enzymes used: BamHI/HindIII. Expected sizes: 2931, 415 bp.

The constructs in pBluescript were then inserted again in the pICH86988 vector along with the rest of the fragments, using the Golden Gate protocol. Additionally, each truncated gene was tagged with YFP (Yellow Fluorescent Protein). Therefore, the plasmids constructed in pICH86988 were: pICH86988:*Bn*RPR1ΔB3:YFP, pICH86988:*Bn*RPR1ΔTFSII:YFP and pICH86988:*Bn*RPR1ΔB3ΔTFSII:YFP.

Moreover, the Golden gate products were also checked via restriction enzyme digestion (figure 13). All of the constructs were digested with BamHI and HindIII restriction enzymes. The expected sizes were 4985,3067, 2569, 1413, 695, 577, 145 bp for pICH86988:*Bn*RPR1ΔB3:YFP, 4538, 3660, 2569, 1413, 577, 145 bp for pICH86988:*Bn*RPR1ΔTFSII:YFP and 4338, 3067, 2569, 1413, 577, 145 bp for pICH86988:*Bn*RPR1ΔB3ΔTFSII:YFP. The plasmid maps can be found at the supplementary data section (supplementary data figure B).

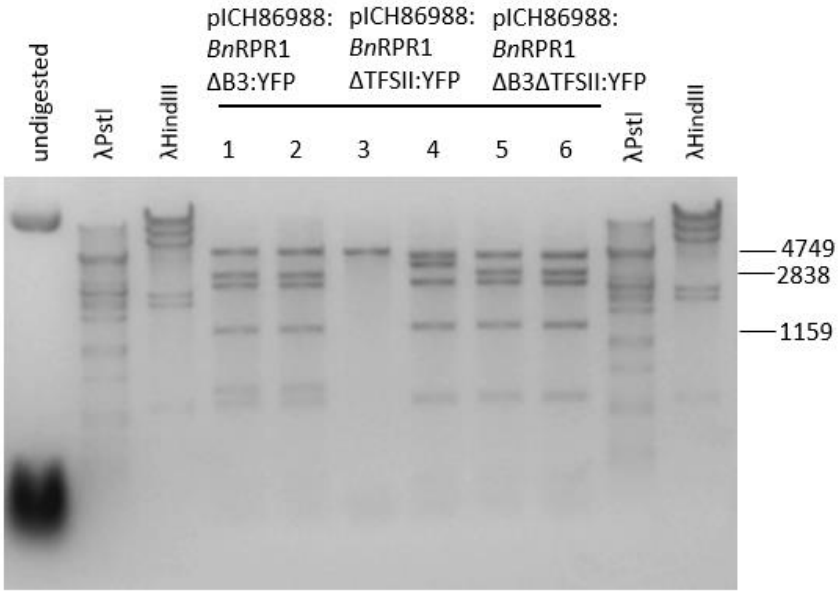

Figure 12. Restriction enzyme digestion results of pICH86988:*Bn*RPR1ΔB3:YFP, pICH86988:*Bn*RPR1ΔTFSII:YFP and pICH86988:*Bn*RPR1ΔB3ΔTFSII:YFP. Restriction enzymes used: BamHI/HindIII. Expected sizes: 4985,3067, 2569, 1413, 695, 577, 145 & 4538, 3660, 2569, 1413, 577, 145 & 4338, 3067, 2569, 1413, 577, 145 bp respectively. Sample number 4 was not taken into consideration.

The transformed *A. tumefaciens* cells with the constructs engineered were used for agroinfiltration assays. The tissue used for this experiment was *N. benthamiana* and *N. tabacum* leaves. The agroinfiltration assay was performed in patches on the leaf surface. *Bn*RPR1:YFP and *Bn*RPR2:mCherry were again overexpressed together as a positive HR control. In order to examine which exact domain of *Bn*RPR1 plays an essential role in the triggering of HR we overexpressed each truncated *Bn*RPR1 NLR along with *Bn*RPR2. In detail, different patches were created on the leaf following the agroinfiltration protocol; *Bn*RPR1ΔB3:YFP, *Bn*RPR1ΔTFSII:YFP and *Bn*RPR1ΔB3ΔTFSII:YFP were co - expressed with *Bn*RPR2:mCherry. This experiment was repeated three times.

The results were analyzed in combination with the positive control (co expression of *Bn*RPR1:YFP and *Bn*RPR2:mCherry) that triggered HR in 48 hours. It is observed that TFSII domain plays an important role in the cause of HR. When the TFSII domain is absent from the *Bn*RPR1 gene HR response was delayed. The absence of the B3 domain led to HR in 48 hours, as the positive control (figures 14, 15).

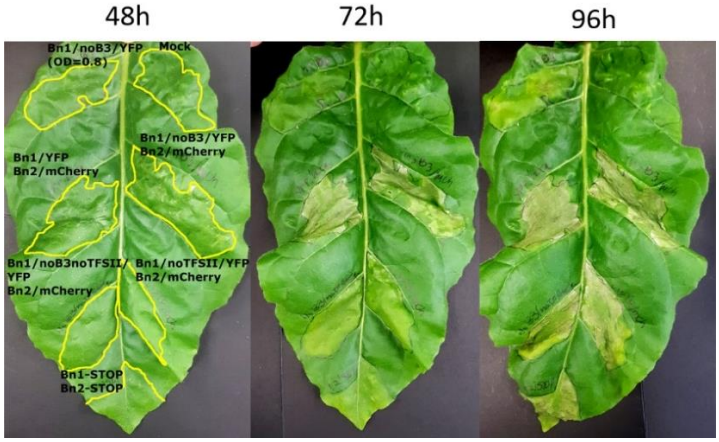

Figure 13. Agroinfiltration results. *Bn*RPR1 co-expressed with *Bn*RPR2 triggers HR, as a positive control. Each truncated NLR, missing the B3 domain, the TFSII domain or both was overexpressed along with *Bn*RPR2. When the TFSII domain was absent from the BnRPR1 gene, HR response was delayed. *N. tabacum* leaves were used for this agroinfiltration assay and the experiment was repeated three times.

Figure 14. Agroinfiltration results. *Bn*RPR1 co-expressed with *Bn*RPR2 triggers HR, as a positive control. Each truncated NLR, missing the B3 domain, the TFSII domain or both was overexpressed along with *Bn*RPR2. When the TFSII domain was absent from the BnRPR1 gene HR response was delayed. *N. benthamiana* leaves were used for this agroinfiltration assay and the experiment was repeated three times.

In order to examine whether the difference in the triggering of HR by each truncated NLR is combined with a different localization of the expressed protein in the plant cell, we conducted some confocal microscopy observations. It has already been shown by Amartolou A. that *BnRPR1* when overexpressed alone is localized in the nucleus, whereas *BnRPR2* is localized in specific spots inside the nucleus, which are speculated to be the nucleoli. When these two genes are overexpressed together, the spots inside the nucleus are also observed.

N. benthamiana leaves were used for this experiment. More specifically, at first, all the truncated NLR genes (BnRPR1ΔB3:YFP, BnRPR1ΔTFSII:YFP and BnRPR1ΔB3ΔTFSII:YFP) were overexpressed in *N. benthamiana* leaves. *Bn*RPR1:YFP was used as a control. 48 hours after the agroinfiltration assays, the samples were observed under the confocal microscope.

Truncated *Bn*RPR1 without the B3 domain was found inside the nucleus, just like *Bn*RPR1. On the contrary, when TFSII domain is absent from *Bn*RPR*1*, the expressed protein seems to be localized mostly in the cytoplasm and less in the nucleus (figure 16).

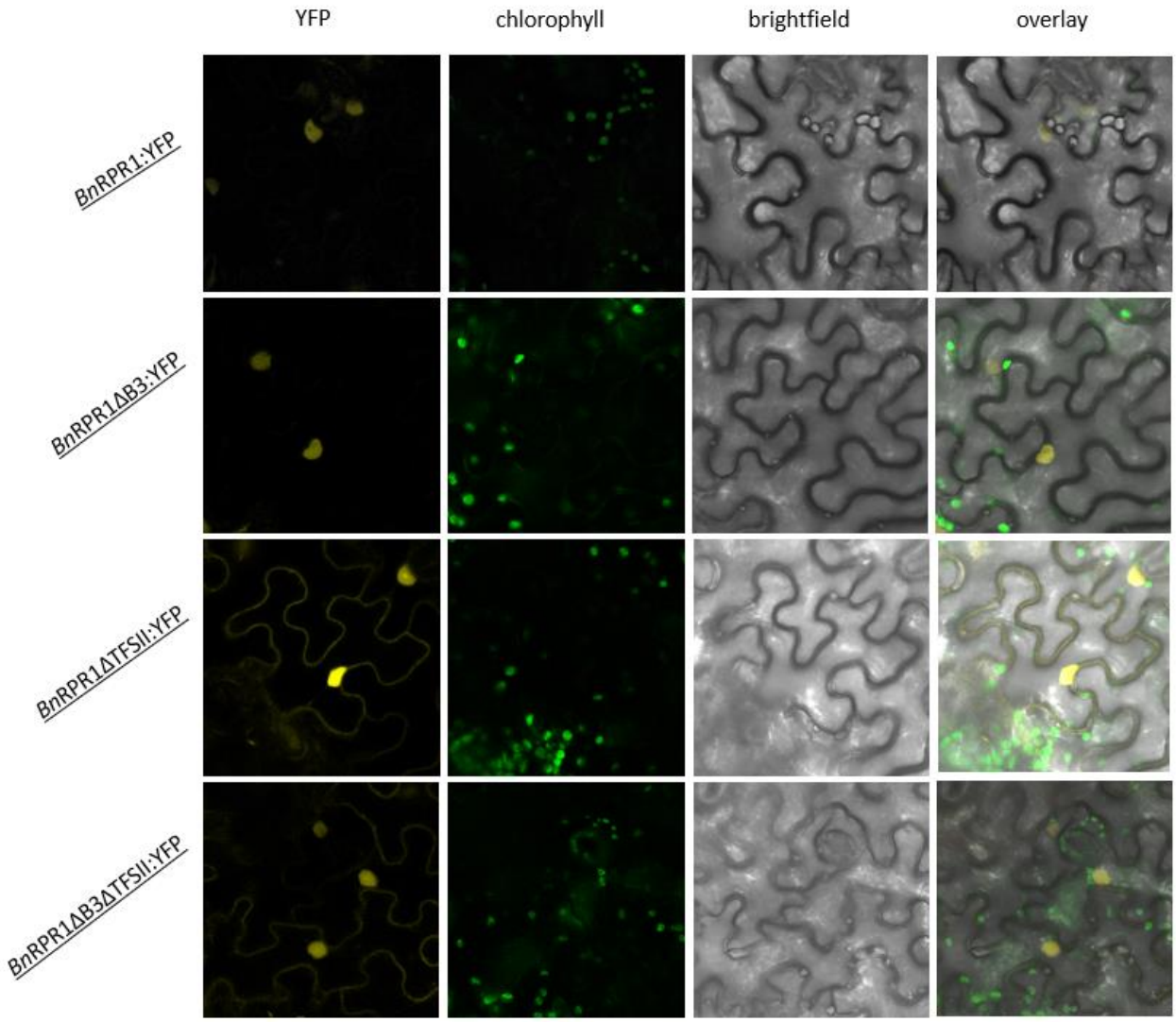

Figure 15. Confocal microscopy results. Observation under the Confocal microscope of *N. benthamiana* leaves 48 hours after the agroinfiltration assays. *Bn*RPR1:YFP was overexpressed alone, as a positive control as it has already been shown to be localized in the nucleus (Amartolou 2019, thesis). *Bn*RPR1ΔB3:YFP, *Bn*RPR1ΔTFSII:YFP and *Bn*RPR1ΔB3ΔTFSII:YFP were also overexpressed each one alone. Truncated *Bn*RPR1 without the B3 domain was found inside the nucleus, just like *Bn*RPR1. On the contrary, when TFSII domain is absent from *Bn*RPR1, the expressed protein seems to be remaining also in the cytoplasm.

Additionally, another experiment was conducted in order to examine if the localization of the truncated *Bn*RPR1 NLRs is altered when each one is co – expressed with *Bn*RPR2. *Bn*RPR1:YFP co – expressed with *Bn*RPR2:mCherry was used as a control. 48 hours after the agroinfiltration assays , the samples were observed again under the confocal microscope.

*Bn*RPR1 along with *Bn*RPR2 create specific spots inside the nucleus, as it was shown by Amartolou A. TFSII domain continues to play an important role in the localization of the *Bn*RPR1 NLR, because when the TFSII domain is absent the protein is localized also in the cytoplasm. Moreover, no spots were detected when TFSII domain was absent (figure 17).

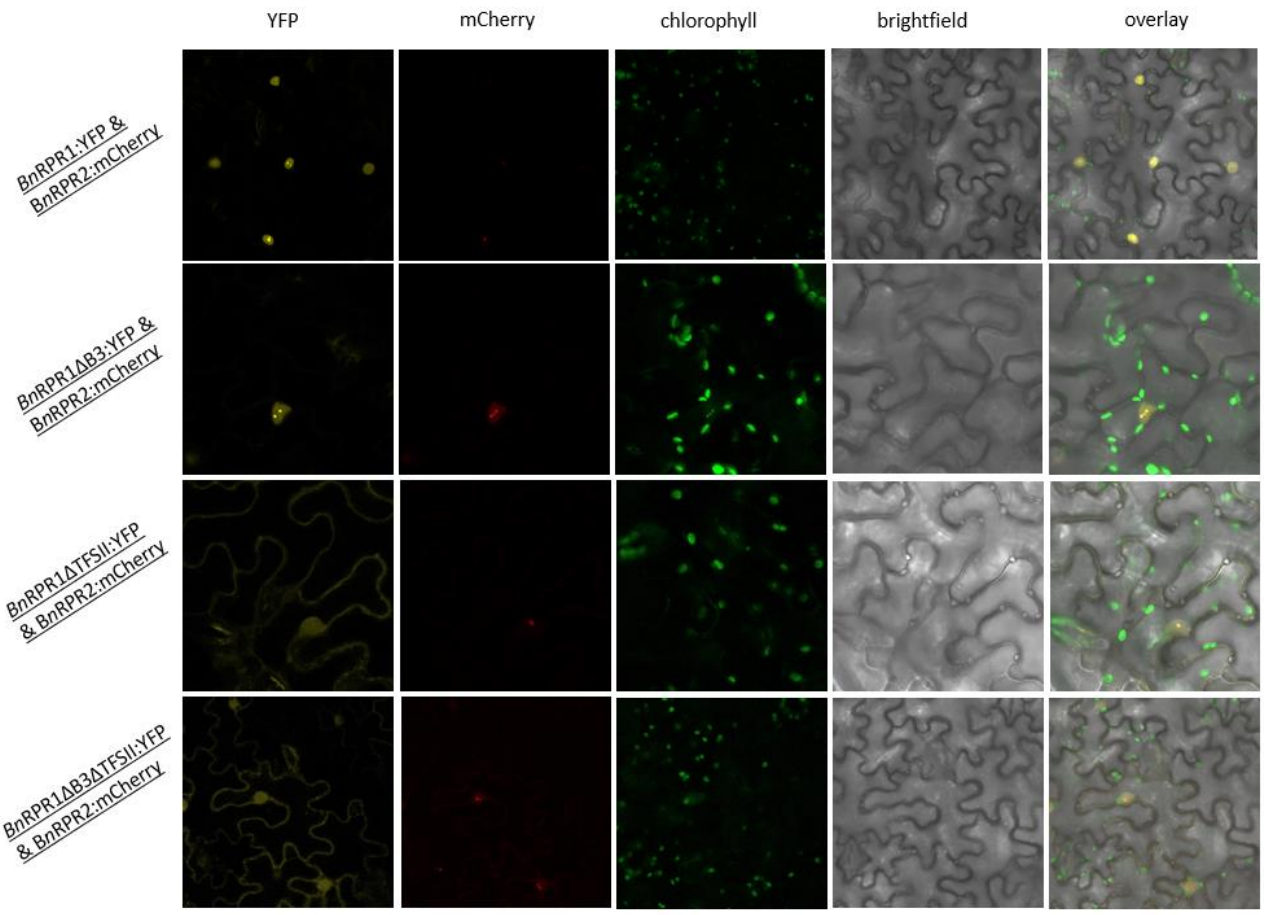

Figure 16. Confocal microscopy results. Observation under the Confocal microscope of *N. benthamiana* leaves 48 hours after the agroinfiltration assays. *Bn*RPR1:YFP was overexpressed along with *Bn*RPR2:mCherry, as a positive control. It has already been shown by Amartolou, 2019 thesis that *Bn*RPR1 is localized in the nucleus, whereas *Bn*RPR2 is localized in specific spots inside the nucleus, which are speculated to be the nucleoli. In this experiment, *Bn*RPR1ΔB3:YFP, *Bn*RPR1ΔTFSII:YFP and *Bn*RPR1ΔB3ΔTFSII:YFP were co – expressed with *Bn*RPR2. TFSII domain continues to play an important role in the localization of the *Bn*RPR1 NLR, because when the TFSII domain is absent the protein is localized also in the cytoplasm and there were no spots created inside the nucleus.

3.3 Role of the overlapping region

Following the same procedure, the role of the overlapping region of *Bn*RPR*1* with *Bn*RPR2 is being studied, in order to examine whether this region plays also a role in the triggering of HR. This overlapping region of *Bn*RPR1 with *Bn*RPR2 coincides with the 5'UTR of the *Bn*RPR1 gene. For this purpose, a construct of *Bn*RPR1 containing the overlapping region needs to be engineered.

The first fragment of the *BnRPR1* gene was amplified including the overlapping region. The PCR product was checked via agarose gel electrophoresis, to verify that the PCR has been correctly performed (figure 18). The expected size was 1921 bp.

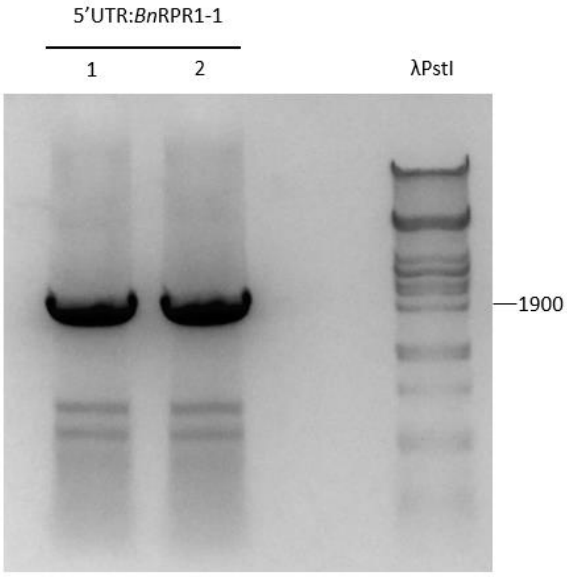

Figure 17. PCR results of 5'UTR:*Bn*RPR1-1. Expected size: 1921 bp.

The amplified fragment was inserted in the pBluescript vector. The ligation product was pBLSKGG:5'UTR:*Bn*RPR1-1. In order to validate that the TA cloning has been performed correctly, the plasmid was digested with restriction enzymes. pBLSKGG:5'UTR:*Bn*RPR1-1 was digested with BamHI/HindIII and the expected sizes were 2931, 1953 bp. The results of the restriction enzyme digestions are shown in figure 19. The plasmid maps designed using the Vector NTI program can be found at the supplementary data section (supplementary data figure A).

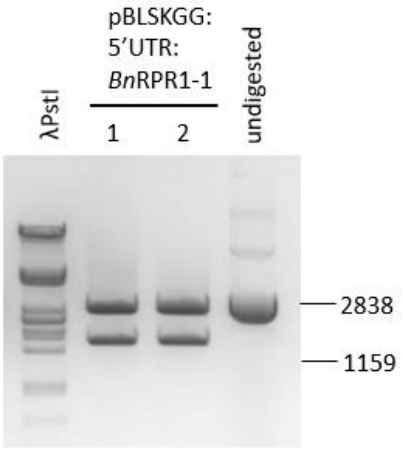

Figure 18. Restriction enzyme digestion results of pBLSKGG:5'UTR:*Bn*RPR1-1. Restriction enzymes used: BamHI/HindIII. Expected sizes: 2931, 1953 bp.

The construct in pBluescript was then inserted again in the pICH86988 vector along with the rest of the fragments, using the Golden Gate protocol. Additionally, this gene was also tagged with YFP (Yellow Fluorescent Protein). Therefore, the plasmids constructed in pICH86988 was: pICH86988:5'UTR:*Bn*RPR1:YFP. This Golden gate products was also checked via restriction enzyme digestion (figure 20). pICH86988:5'UTR:BnRPR1:YFP was digested with BamHI and ApaII restriction enzymes and the expected sizes were 5166, 4958, 3399, 1110 bp. The plasmid map can be found at the supplementary data section (supplementary data figure B).

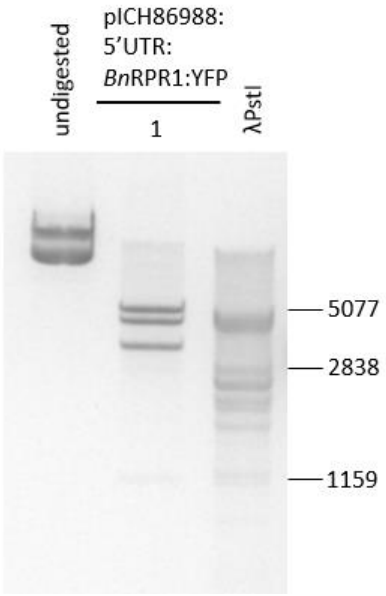

Figure 19. Restriction enzyme digestion results of pICH86988:5'UTR:*Bn*RPR1:YFP. Restriction enzymes used: BamHI/ApaII. Expected sizes: 5166, 4958, 3399, 1110 bp.

The transformed *A. tumefaciens* cells with the constructs engineered were used for agroinfiltration assays. The tissue used for this experiment was *N. benthamiana* leaves. The agroinfiltration assay was performed in patches on the leaf surface. *Bn*RPR1:YFP and *Bn*RPR2:mCherry were again overexpressed together as a positive HR control.

In order to examine if the overlapping region of *Bn*RPR1 with *Bn*RPR2 affects the trigger of HR we overexpressed the *Bn*RPR1 NLR with the 5'UTR along with *Bn*RPR2. In detail, different patches were created on the leaf following the agroinfiltration protocol; *Bn*RPR1:YFP co – expressed with BnRPR2:mCherry as a positive HR control and 5'UTR:BnRPR1:YFP co – expressed with BnRPR2:mCherry. This experiment was repeated three times.

The results were analyzed in combination with the positive control (co expression of *Bn*RPR1:YFP and *Bn*RPR2:mCherry) that triggered HR in 48 hours. It is observed that overlapping region also plays an important role in the triggering of HR. When the overlapping region is absent from the *Bn*RPR1 gene no HR was detected, or it was triggered after 72 hours (figure 21).

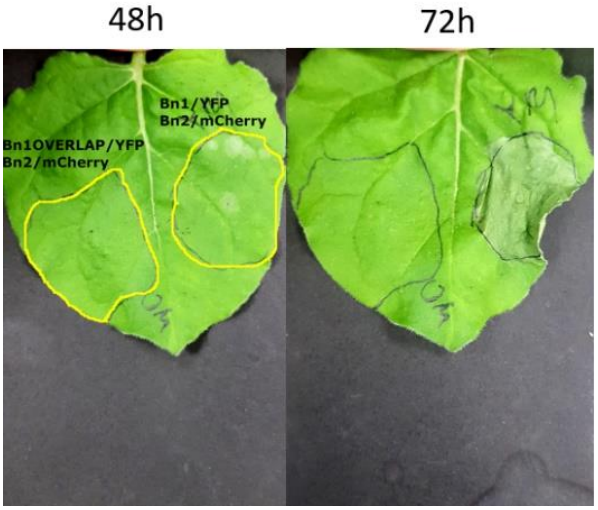

Figure 20. Agroinfiltration results. *Bn*RPR1:YFP co-expressed with *Bn*RPR2:mCherry triggers HR, as a positive control. 5'UTR:*Bn*RPR1:YFP was overexpressed along with *Bn*RPR2. When the overlapping region was expressed HR was not triggered. *N. benthamiana* leaves were used for this agroinfiltration assay and the experiment was repeated three times.

In order to examine whether the difference in the triggering of HR by the presence of the overlapping region is combined with a different localization of the expressed protein in the plant cell, we conducted some confocal microscopy observations. It has already been shown by Amartolou A. that *BnRPR1* when overexpressed alone is localized in the nucleus, whereas *BnRPR2* is localized in specific spots inside the nucleus, which are speculated to be the nucleoli.

N. benthamiana leaves were used for this experiment. More specifically, 5'UTR:BnRPR1:YFP was overexpressed in *N. benthamiana* leaves. *Bn*RPR1:YFP with was used as a control. 48 hours after the agroinfiltration assays, the samples were observed under the confocal microscope (figure 22).

Confocal microscopy observations revealed that when *Bn*RPR1 is expressed with the overlapping region its localization changes. In fact, the protein seems to be found not only in the nucleus but also in the cytoplasm.

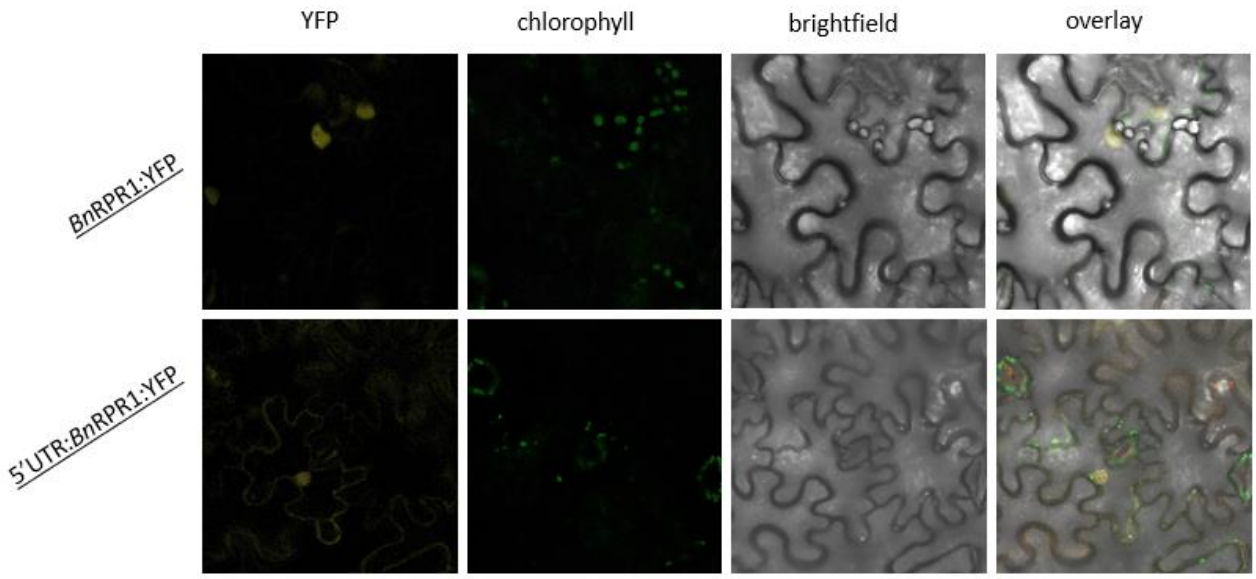

Figure 21. Confocal microscopy results. Observation under the Confocal microscope of *N. benthamiana* leaves 48 hours after the agroinfiltration assays. *Bn*RPR1:YFP was overexpressed alone, as a positive control as it has already been shown to be localized in the nucleus (Amartolou 2019, thesis). 5'UTR:*Bn*RPR1:YFP *was* also overexpressed. When the overlapping region is expressed with the *Bn*RPR1 NLR, the expressed protein seems to be localized in the nucleus and also in the cytoplasm.

Additionally, another experiment was conducted in order to examine if the localization of the *Bn*RPR1 NLR, which is expressed along with the overlapping region, is altered when it is co – expressed with *Bn*RPR2. *Bn*RPR1:YFP co – expressed with *Bn*RPR2:mCherry was used as a control. 48 hours after the agroinfiltration assays, the samples were observed again under the confocal microscope.

*Bn*RPR2 seems to be localized in all the samples at specific spots inside the nucleus, as it was shown by Amartolou A. The overlapping region continues to play an important role in the localization of the *Bn*RPR1 NLR, because when it is present the protein is localized also in the cytoplasm (figure 23).

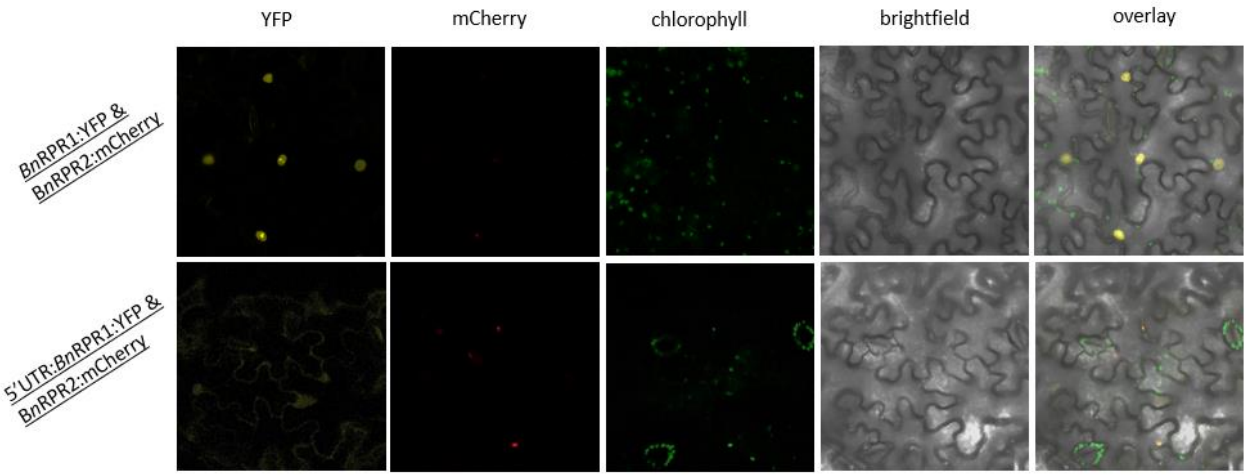

Figure 22. Confocal microscopy results. Observation under the Confocal microscope of N. benthamiana leaves 48 hours after the agroinfiltration assays. BnRPR1:YFP was overexpressed along with BnRPR2:mCherry, as a positive control. It has already been shown by Amartolou, 2019 thesis that BnRPR1 is localized in the nucleus, whereas BnRPR2 is localized in specific spots inside the nucleus, which are speculated to be the nucleoli. In this experiment, 5'UTR:*Bn*RPR1:YFP was co – expressed with BnRPR2. The overlapping region continues to play an important role in the localization of the BnRPR1 NLR, because when it is present the protein is localized also in the cytoplasm.

3.4 Interaction with virulence effectors

The *BnRPR1* NLR receptor was analyzed for its interaction with specific virulence effectors from the Turnip Mosaic Virus (TuMv), a virus that infects the *B. napus* plants. The effectors selected for this study were a helper component protein (HcPro) and a viral genome-linked protein (VPg) from the TuMV.

The helper component protein was discovered by Pirone and Thornbury in 1984. This viral protein received this name because it was a protein with an unknown function and source which was detected in infected plants. It was speculated that it had a role in the transmission of the potyviruses via the aphid mouthparts (Pirone & Thornbury , 1984). Until now, HcPro has been shown to have three major functions: the transmission of the virus to the host plant, participation in the maturation of the viral polyprotein complex, the suppression of the RNA silencing defense mechanism of the host plant and the interaction with the host plant defense factors (Valli et al., 2018). The viral genome-linked protein is a protein attached to the 5' end of the viral positive sense RNA. VPg plays an important role in the virus replication cycle as it has been shown that it also interacts with many host proteins and factors (Jiang & Laliberté, 2011). Therefore, it was speculated that these two effectors may interact with the *Bn*RPR1 NLR defence receptor.

The interaction between the *BnRPR1* NLR receptor and the virulence effectors is being tested, at first, through Yeast 2 Hybrid assays. This method relies on the fact that the DNA-binding domain (BD) and transcriptional activation domain (AD) of the *S. cerevisiae* transcription factor GAL4 can be separated. The

BD is attached to one gene (bait) and the AD is attached to the other gene (prey). When these two proteins interact, the transcription process is activated and yeast can successfully grow in media that is missing adenine (Fields & Song , 1989). These experiments were also repeated three times each.

For this purpose, certain constructs were designed in order to check for interactions between the HcPro or VPg virulence effectors with the two specific, integrated domains of *Bn*RPR1, B3 and TFSII. The final vectors will be pGBKT7 for B3 and TFSII domains and pGADT7 for the virulence effectors. These constructs will be used for the Y2H assays. The procedure for the engineering of the constructs was the same. The effector fragments were amplified from the TuMv total genome and the B3 domain was amplified using as a template already existing isolated plasmids containing the *Bn*RPR1 gene, using specific primers, via the PCR protocol (supplementary data table 1). More specifically, each reverse primer of HcPro and VPg contained a stop codon. The PCR products were checked via agarose gel electrophoresis, to verify that the PCR has been correctly performed (figure 24). The expected sizes were 1402, 605 and 346 bp, respectively.

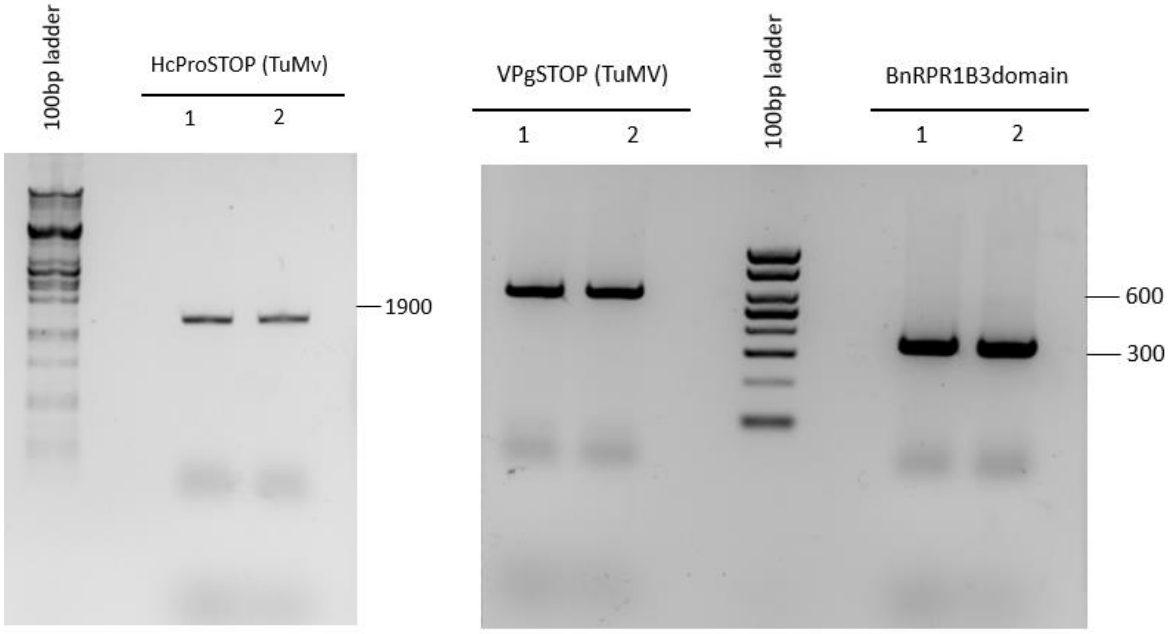

Figure 23. PCR results of HcProSTOP, VPgSTOP and *Bn*RPR1B3domain. Expected sizes: 1402, 605 and 346 bp.

The amplified fragments were inserted in the pBluescript vector. The ligation products were pBLSKGG:HcProSTOP, pBLSKGG:VPgSTOP and pBLSKGG:BnRPR1B3domain. In order to validate that the TA cloning has been performed correctly, the plasmids were digested with restriction enzymes. pBLSKGG:HcProSTOP was digested with BamHI/HindIII and the expected sizes were 2931, 1371, 38, 25 bp. pBLSKGG:VPgSTOP was digested with BamHI/HindIII and the expected sizes were 2931, 385, 251 bp. pBLSKGG:*Bn*RPR1B3domain was digested with BamHI/HindIII and the expected sizes were 2931, 342, 36 bp. The results of the restriction enzyme digestions are shown in figures 25 and 26. The plasmid maps

designed using the Vector NTI program can be found at the supplementary data section (supplementary data figure A).

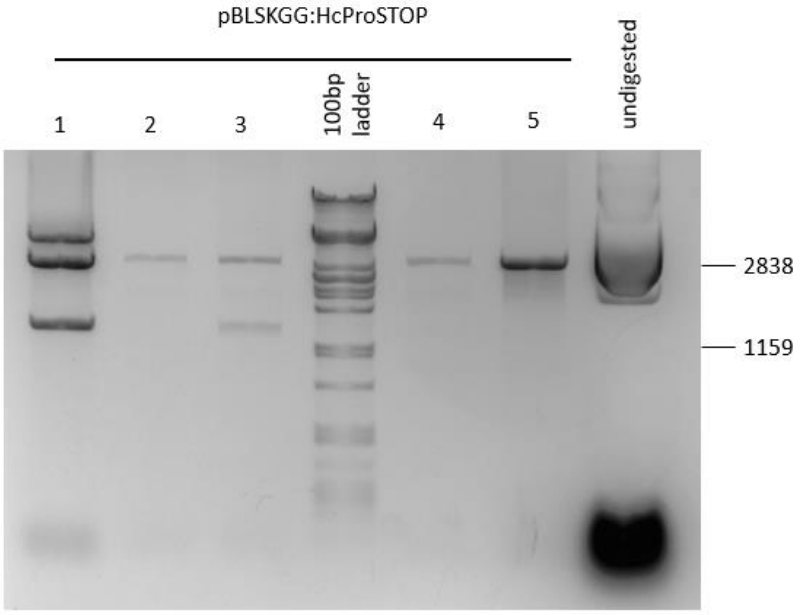

Figure 24. Restriction enzyme digestion results of pBLSKGG:HcProSTOP. Restriction enzymes used: BamHI/HindIII. Expected sizes: 2931, 1371, 38, 25 bp. Samples 2, 4, 5 were not taken into consideration.

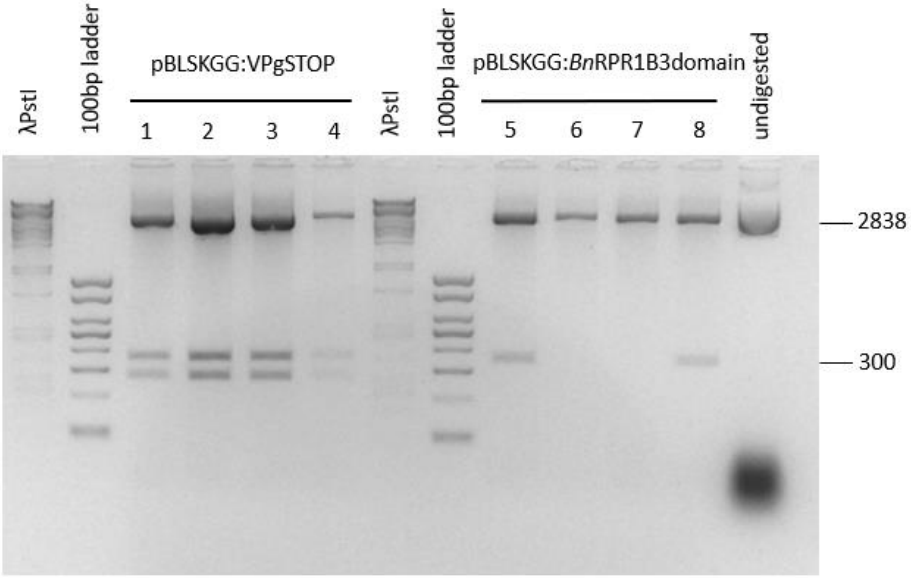

Figure 25. Restriction enzyme digestion results of pBLSKGG:HcProSTOP and pBLSKGG:*Bn*RPR1B3domain. Restriction enzymes used: BamHI/HindIII. Expected sizes: 2931, 385, 251 bp and 2931, 342, 36 bp, respectively. Samples 6, 7 were not taken into consideration.

The HcPro and VPg fragments were then inserted in the vector pGAKT7 and the B3 domain fragment was inserted in pGBDT7 vector. pGBKT7 vector is designed to express the BD domain of the GAL4 pathway and the bait protein (B3 ot TFSII). Whereas the pGADT7 vector includes the AD domain and the prey protein (HcPro or VPg). The ligation products were: pGADT7:HcProSTOP, pGADT7:VPgSTOP and pGBKT7:BnRPR1B3domain. The plasmids were checked via restriction enzyme digestion after the ligation protocol (figures 27, 28, 29). pGADT7:HcProSTOP was digested with EcoRV and the expected sizes were 5694, 1807, 1130, 645 bp. pGADT7:VPgSTOP was digested with HindIII and the expected sizes were 4938, 1498, 1088, 295 bp. pGBKT7:*Bn*RPR1B3domain was digested with HindIII and the expected sizes were 4938, 1498, 830, 295 bp. The plasmid maps designed using the Vector NTI program can be found at the supplementary data section (supplementary data figures C, D). pGBKT7:*TFSII* construct was provided by Michalopoulou Vasiliki.

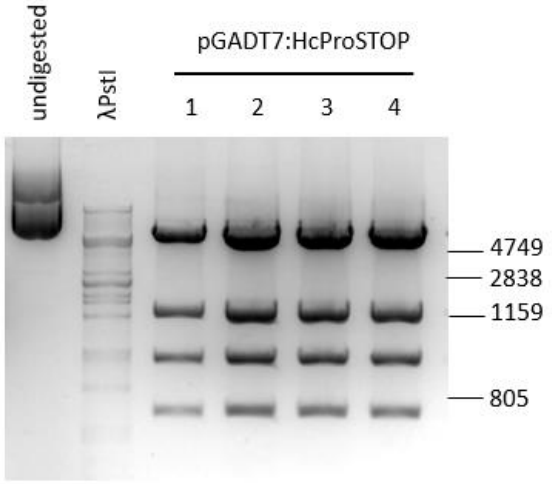

***Figure 26*.** Restriction enzyme digestion results of pGADT7:HcProSTOP. Restriction enzymes used: EcoRV. Expected sizes: 5694, 1807, 1130, 645 bp.

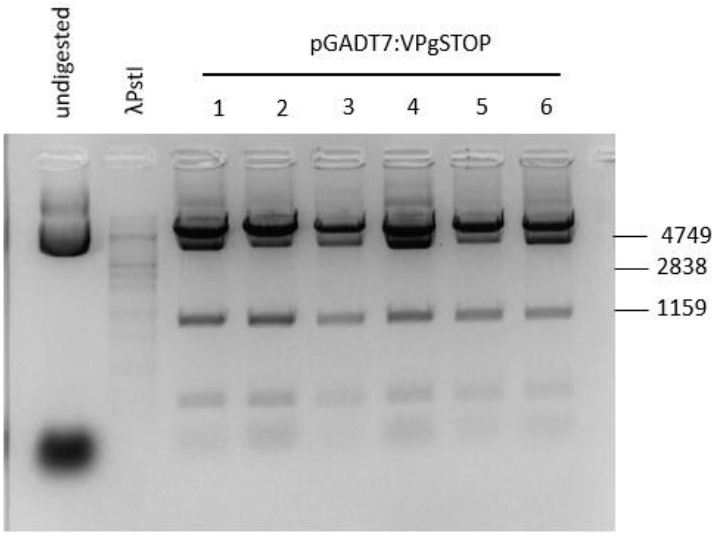

Figure 27. Restriction enzyme digestion results of pGADT7:VPgSTOP. Restriction enzymes used: HindIII. Expected sizes: 4938, 1498, 1088, 295 bp.

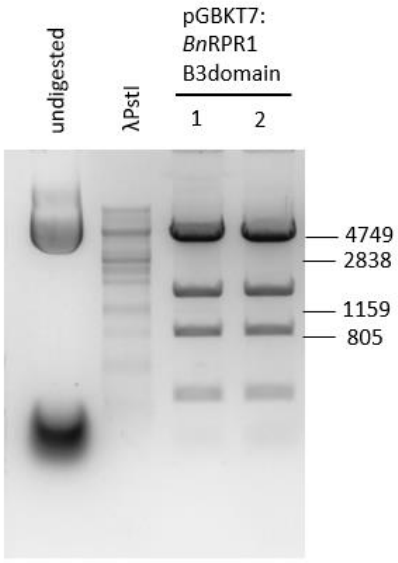

Figure 28. Restriction enzyme digestion results of pGBKT7:*Bn*RPR1B3domain. Restriction enzymes used: HindIII. Expected sizes: 4938, 1498, 830, 295 bp.

After the constructs were engineered the yeast 2 hybrid assays were conducted. More specifically, yeast colonies carrying the different constructs were grown in media containing adenine, as a control. As a positive control, pGADT7:AvrRPS4 with pGBKT7:WRKY was used. Empty pGADT7:RFP and pGBKT7:RFP

vectors were used as a negative control. Growth of yeast colonies on media lacking adenine will reveal the possible interactions.

The Yeast 2 Hybrid results indicated only an interaction of HcPro with the TFSII domain (figure 30). VPg did not interact with any of the domains of *BnRPR1,* as can be regarded by the Yeast 2 Hybrid assays.

	-L -W	-L -W -A
positive control		
PGBKT7:BnB3 – PGADT7:HcPro		
PGBKT7:BnB3 – PGADT7:VPg		
PGBKT7:TFSII - PGADT7:HcPro		
PGADT7:VPg - PGBKT7:TFSII		
negative control		

Figure 29. Yeast 2 Hybrid results. The results showed an interaction of HcPro with the TFSII domain of the *Bn*RPR1 NLR receptor when yeast was grown on a plate lacking adenine. As a positive control, pGADT7:AvrRPS4 with pGBKT7:WRKY was used. Empty pGADT7:RFP and pGBKT7:RFP vectors were used as a negative control

Furthermore, this positive protein interaction of HcPro with the TFSII domain of *Bn*RPR1 was also tested through Bimolecular fluorescence complementation (BiFc). For this purpose certain constructs needed to be engineered. pICH86988:*Bn*RPR1:nVenus construct was provided by Mermigka Glykeria. HcPro was amplified from the whole TuMv genome, using the PCR protocol. The reverse primer did not contain a stop codon (supplementary data table 1). The PCR product was checked via agarose gel electrophoresis, to verify that the PCR has been correctly performed (figure 30). The expected size was 1402 bp.

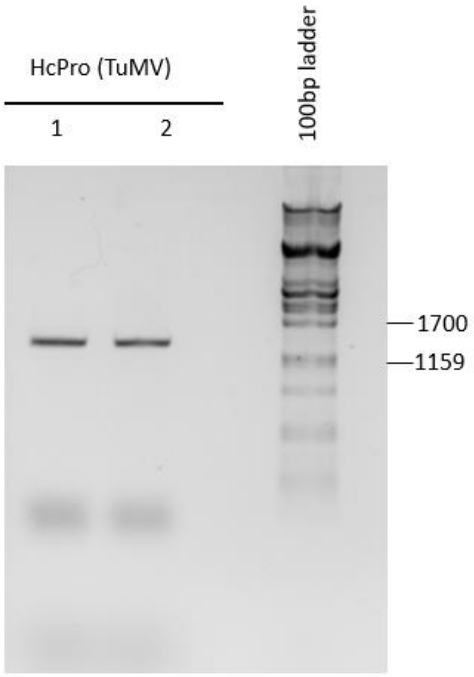

Figure 30. PCR results of HcPro. Expected size: 1402 bp.

The amplified fragment was inserted in the pBluescript vector. The ligation product was pBLSKGG:HcPro. In order to validate that the TA cloning has been performed correctly, the plasmid was digested with restriction enzymes. pBLSKGG:HcPro was digested with HindIII and the expected sizes were 2944, 1371 bp. The results of the restriction enzyme digestions are shown in figure 31. The plasmid maps designed using the Vector NTI program can be found at the supplementary data section (supplementary data figure A).

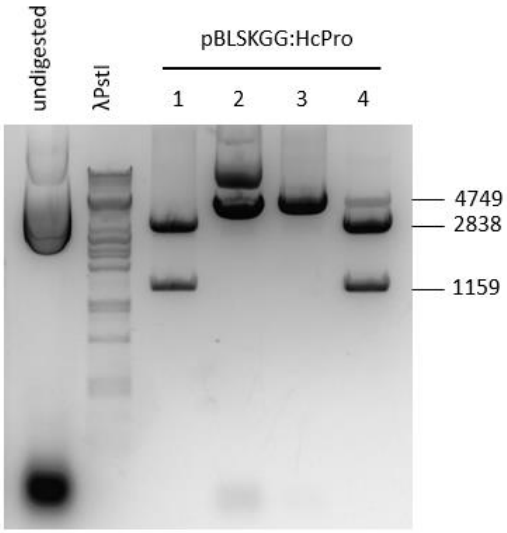

Figure 31. Restriction enzyme digestion results of pBLSKGG:HcPro. Restriction enzyme used: HindIII. Expected sizes: 2944, 1371 bp. Samples 2, 3 were not taken into consideration.

The fragments were then inserted in the pICH86988 vector using the Golden Gate protocol. The Golden Gate products were: pICH86988:HcPro:mNeon and pICH86988:HcPro:cCFP (for the BiFc assays). The plasmids were checked via restriction enzyme digestion (figure 32). pICH86988:HcPro:mNeon was digested with HindIII and the expected sizes were 3982, 3062, 2787, 740 bp. pICH86988:HcPro:cCFP was digested with HindIII and the expected sizes were 3982, 3352, 2787 bp. The plasmid maps designed using the Vector NTI program can be found at the supplementary data section (supplementary data figure B).

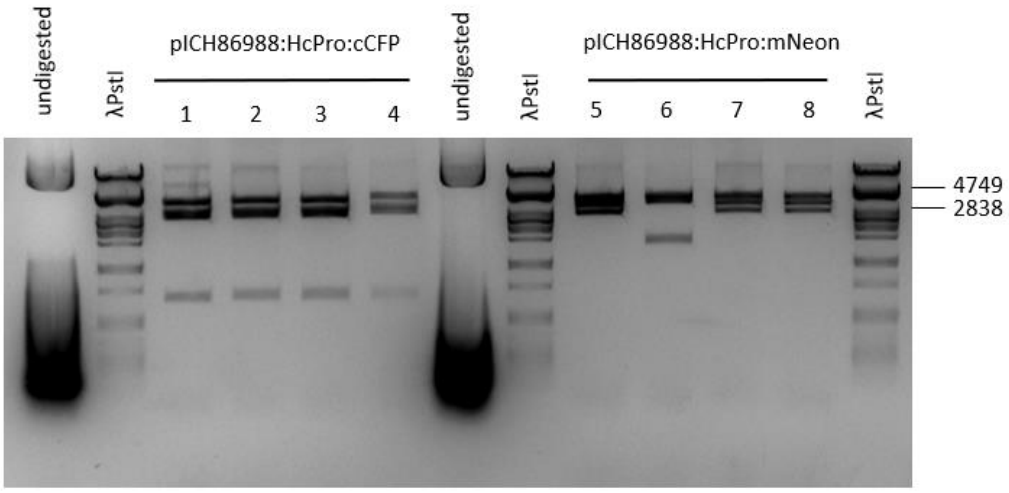

Figure 32. Restriction enzyme digestion results of pICH86988:HcPro:mNeon and pICH86988:HcPro:cCFP. Restriction enzyme used: HindIII. Expected sizes: 3982, 3062, 2787, 740 bp and 3982, 3352, 2787 bp, respectively. Samples 6, 7 were not taken into consideration.

The correct plasmids were isolated and used for the transformation of *A. tumefaciens* (C58C1) competent cells. The transformed *A. tumefaciens* cells were used for agroinfiltration assays. The tissue used for this experiment was *N. benthamiana* leaves. The agroinfiltration assay was performed in patches on the leaf surface. 48 hours after the agroinfiltration assays, the samples were observed under the confocal microscope.

HcPro:mNeon overexpressed alone was spotted only in the cytoplasm (figure 33). In order to verify the interaction between the HcPro virulence effector and the *Bn*RPR1 NLR receptor we conducted this BiFc experiment. HcPro:cCFP co – expressed with *Bn*RPR1:nVenus revealed an interaction between these two proteins and the complex was found in the nucleus (figure 34). In the BiFc assay, *Bn*RPR1:YFP with HcPro:cCFP was used as a control, and it is localized in the nucleus.

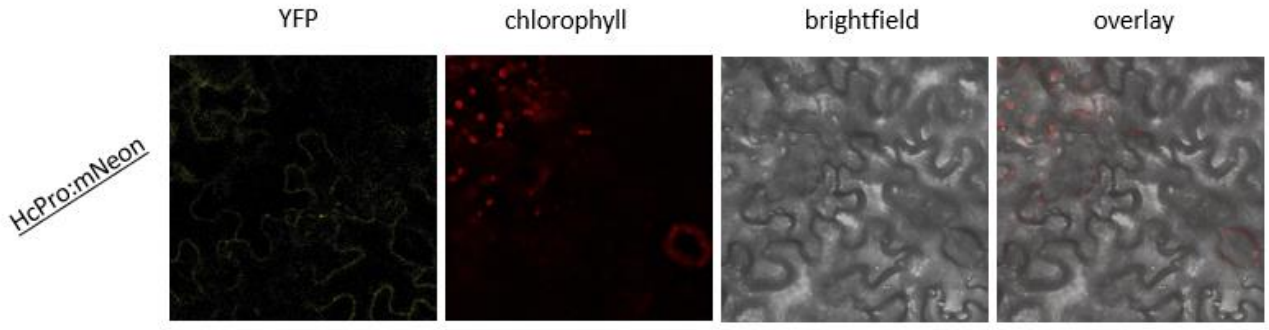

Figure 33. Confocal microscopy results. Observation under the Confocal microscope of *N. benthamiana* leaves 48 hours after the agroinfiltration assays. In this experiment, HcPro:mNeon was overexpressed alone and it is observed to be localized in the cytoplasm.

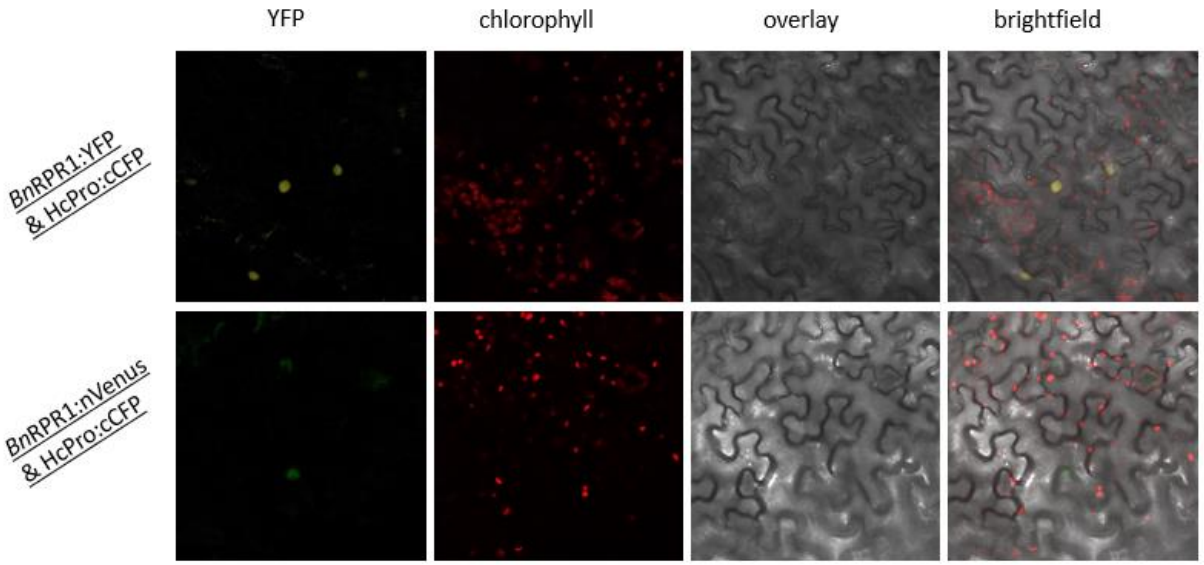

Figure 34. Bimolecular fluorescence complementation (BiFc) assay. Observation under the Confocal microscope of N. benthamiana leaves 48 hours after the agroinfiltration assays. BnRPR1:YFP with HcPro:cCFP was used as a control, and it was localized in the nucleus. HcPro:cCFP co – expressed with BnRPR1:nVenus revealed an interaction between these two proteins and the complex was found in the nucleus.

4. Discussion

A new pair of NLR receptors, *Bn*RPR1 and *Bn*RPR2 has been identified and studied in the present master thesis. It is already been shown by Amartolou A. that when this pair is overexpressed in model plant leaves, without the presence of virulence effectors, hypersensitive response is triggered. The pair's role tried to be analyzed by examining different, important domains of *BnRPR1* that work as integrated domains (IDs), during the recognition of virulence effectors. It is shown that, TFSII domain is crucial to the triggering of hypersensitive response in plant leaves. A reason may be its containing of a Nuclear Localization Signal (NLS), a signal that is responsible for the localization of the protein into the nucleus. When TFSII is absent, the NLR pair cannot be transferred to the nucleus and, thus, it cannot trigger HR to the plant. On the other hand, the absence of the B3 domain has no effect to its function or its localization in the plant cell. Additionally, another domain that plays a significant role is the overlapping region of the two NLRs, that coincides with their 5' UTR. More specifically, when *Bn*RPR1 is expressed along with the overlapping region, it cannot be fully transferred to the nucleus and again HR is delayed or not triggered. It is speculated that this overlapping region may constitute a target of silencing factors, but more research needs to be conducted for this hypothesis to be proven. Lastly, as for the virulence effectors and their interaction with the NLR pair, it is demonstrated that the helper component protein from the Turnip Mosaic virus interacts with the *Bn*RPR1 NLR and specifically with its TFSII domain. Therefore, this NLR may provide resistance to the Turnip Mosaic Virus.

This genetically linked NLR pair, *Bn*RPR1 and *Bn*RPR2 seems to be of great importance. It is still unclear why it triggers hypersensitive response without the presence of any virulence effectors. This study demonstrates and analyzes the role of important domains of *Bn*RPR1*,* as a way to clarify the role of the NLR pair. Further studies need to be carried out in order to understand deeply the function of this receptor pair and its importance in plant defense mechanisms.

References

Adachi, H., Derevnina, L., & Kamoun, S. (2019). NLR singletons, pairs, and networks: evolution, assembly, and regulation of the intracellular immunoreceptor circuitry of plants. *Current Opinion in Plant Biology*, 50:121-131.

Baggs, E., Dagdas, G., & Krasileva, K. V. (2017). NLR diversity, helpers and integrated domains: making sense of the NLR IDentity. *Current Opinion in Plant Biology*, 38:59–67.

Boller, T., & Felix, G. (2009). A Renaissance of Elicitors: Perception of Microbe-Associated Molecular Patterns and Danger Signals by Pattern-Recognition Receptors. *The Annual Review of Plant Biology* , 60:379–406.

Bonardi, V., Cherkis, K., Nishimura, M. T., & Dangl, J. L. (2012). A new eye on NLR proteins: focused on clarity or diffused by complexity? *Current Opinion in Immunology*, 24(1):41-50.

Brader, G., Compant, S., Mitter, B., Trognitz, F., & Sessitsch, A. (2014). Metabolic potential of endophytic bacteria. *Current Opinion in Biotechnology*, 27:30-37.

Brückner, A., Polge, C., Lentze, N., Auerbach, D., & Schlattner, U. (2009). Yeast Two-Hybrid, a Powerful Tool for Systems Biology. *International Journal of Molecular Sciences*, 10:2763-2788.

Cai, Q., Qiao, L., Wang, M., He, B., Lin, F.-M., Palmquist, J., . . . Jin, H. (2018). Plants send small RNAs in extracellular vesicles to fungal pathogen to silence virulence genes. *Plant Science*, 360:1126–1129.

Cesari, S. (2017). Multiple strategies for pathogen perception by plant immune receptors. *New Phytologist*, 219:17-24.

Chiang, Y.-H., & Coaker, G. (2015). Effector Triggered Immunity: NLR Immune Perception and Downstream Defense Responses. *The Arabidopsis Book*, 1-11.

Chomczynski, P., & Sacchi, N. (1987). Single-step method of RNA isolation by acid guanidinium thiocyanate-phenol-chloroform extraction. *Analytical Biochemistry*, 162:156-159.

Costantini, L. M., Fossati, M., Francolini, M., & Snapp, E. (2012). Assessing the Tendency of Fluorescent Proteins to Oligomerize Under Physiologic Conditions. *Traffic*, 13:643–649.

Cui, H., Tsuda, K., & Parker, J. E. (2015). Effector-Triggered Immunity: From Pathogen Perception to Robust Defense. *Annual Review of Plant Biology*, 66:487-511.

Dodds, P. N., & Rathjen, J. P. (2010). Plant immunity: towards an integrated view of plant–pathogen interactions. *nATuRE REvIEwS | Genetics* , 11:539-548.

Eitas, K. T., & Dangl, L. J. (2010). NB-LRR proteins: pairs, pieces, perception, partners,. *Current Opinion in Plant Biology*, 13:472–477.

Erwig, J., Ghareeb, H., Kopischke, M., Hacke, R., Matei, A., Petutschnig, E., & Lipka, V. (2017). Chitin-induced and CHITIN ELICITOR RECEPTOR KINASE1 (CERK1) phosphorylation-dependent endocytosis of Arabidopsis thaliana LYSIN MOTIF-CONTAINING RECEPTOR-LIKE KINASE5 (LYK5). *New Phytologist*, 215:382-396.

Fields, S., & Song , O. (1989). A novel genetic system to detect protein-protein interactions. *Nature*, 340:245–246.

Flor, H. H. (1971). Current Status of the Gene-For-Gene Concept. *Annual Review of Phytopathology*, 9:275-296.

Gassmann, W., Hinsch, M. E., & Staskawicz, B. J. (1999). The Arabidopsis RPS4 bacterial-resistance gene is a member of the TIR-NBS-LRR family of disease-resistance genes. *The Plant Journal*, 20(3):26-277.

Grasser, M., Kane, C. M., Merkle, T., Melzer, M., Emmersen, J., & Grassser, K. D. (2009). Transcript Elongation Factor TFIIS Is Involved in Arabidopsis Seed Dormancy. *Journal of Molecular Biology*, 386:598–611.

Greenberg, J. T. (1996). Programmed cell death: a way of life for plants. *PNAS*, 93:12094-12097.

Han, G.-Z. (2018). Origin and evolution of the plant immune system. *New Phytologist*, 222:70-83.

Jiang, J., & Laliberté, J.-F. (2011). The genome-linked protein VPg of plant viruses — a protein with many partners. *Current Opinion in Virology*, 1(5):347-354.

Jones, J. D., & Dangl, J. L. (2006). The plant immune system. *Nature*, 444:323-329.

Maekawa, T., Kracher, B., Saur, I. M., Yoshikawa-Maekawa, M., Kellner, R., Pankin, A., . . . Schulze-Lefert, P. (2019). Subfamily-Specific Specialization of RGH1/MLA Immune Receptors in Wild Barley. *Molecular Plant-Microbe Interactions*, 32(1):107–119.

Maekawa, T., Kufer, T. A., & Schulze-Lefert, P. (2011). NLR functions in plant and animal immune systems: so far and yet so close. *Nature Immunology*, 12:818-826.

Meng, X., & Zhang, S. (2013). MAPK Cascades in Plant Disease Resistance Signaling. *Annual Review of Phytopathology*, 51:12.1–12.22.

Moffett, P., Farnham, G., Peart, J., & Baulcombe, D. C. (2002). Interaction between domains of a plant NBS–LRR protein in disease resistance-related cell death. *The EMBO Journal*, 21:4511-4519.

Monaghan, J., & Zipfel, C. (2012). Plant pattern recognition receptor complexes at the plasma. *Current Opinion in Plant Biology*, 15:349–357.

New England Biolabs Inc. (2019). Retrieved from https://www.neb.com/products/r0535-bsai#Product%20Information_Product%20Notes

Nicaise, V., Roux, M., & Zipfel, C. (2009). Recent Advances in PAMP-Triggered Immunity against Bacteria: Pattern Recognition Receptors Watch over and Raise the Alarm. *Plant Physiology*, 150:1638–1647.

Pirone, T. P., & Thornbury , D. W. (1984). The involvement of a helper component in nonpersistent transmission of plant viruses by aphids. *Microbiological sciences*, 8:191-193.

Romanel, E. A., Schrago, C. G., Counago, R. M., Russo, C. A., & Alves-Ferreira, M. (2009). Evolution of the B3 DNA Binding Superfamily: New Insights into REM Family Gene Diversification. *PLoS ONE*, 4:e5791.

Sarris, P. F., Duxbury, Z., Huh, S. U., Ma, Y., Segonzac, C., Sklenar, J., . . . Jones, J. D. (2015). A Plant Immune Receptor Detects Pathogen Effectors that Target WRKY Transcription Factors. *Cell*, 161:1089–1100.

Takken, F. L., & Goverse, A. (2012). How to build a pathogen detector: structural basis of NB-LRR function. *Current Opinion in Plant Biology*, 15: 375–384.

Takken, F. L., Albrecht, M., & Tameling, W. I. (2006). Resistance proteins: molecular switches of plant defence. *Current Opinion in Plant Biology*, 9(4):383-390.

Tsuda, K., & Katagiri, F. (2010). Comparing signaling mechanisms engaged in pattern-triggered and effector-triggered immunity. *Current Opinion in Plant Biology*, 13:459-465.

Valli, A. A., Gallo, A., Rodamilans, B., Lopez-Moya, J., & Garcia, J. (2018). The HCPro from the Potyviridae family: an enviable multitasking Helper Component that every virus would like to have. *Molecular Plant Pathology*, 19(3):744–763.

Wang, C.-l. A., Gunc, G., Forwood, J. K., Teh, T., Catanzariti, A.-M., Lawrence, G. J., . . . Kobe, B. (2007). Crystal Structures of Flax Rust Avirulence Proteins AvrL567-A and -D Reveal Details of the Structural Basis for Flax Disease Resistance Specificity. *The Plant Cell*, 19: 2898–2912.

Yeh, Y.-H., Panzeria, D., Kadota, Y., Huang, Y.-C., Huang, P.-Y., Tao, C., . . . Zimmerli, L. (2016). The Arabidopsis malectin-like/LRR-RLK IOS1 is critical for BAK1-dependent and BAK1-independent pattern-triggered immunity. *Plant Cell*, 28:1701-1721.

Zhang, R., Zheng, F., Wei, S., Zhang, S., Li, G., Cao, P., & Zhao, S. (2019). Evolution of Disease Defense Genes and Their Regulators in Plants. *International Journal of Molecular Sciences*, 20(2):335.

Supplementary data

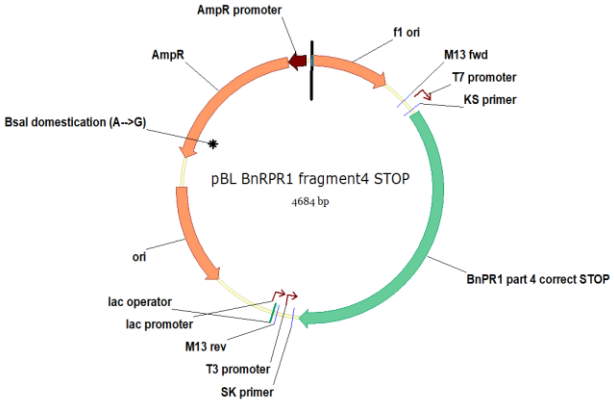

a.

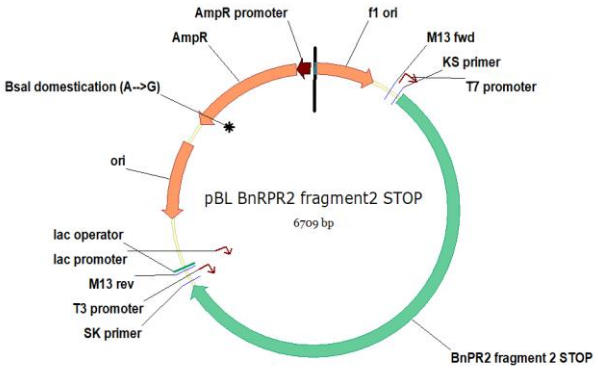

b.

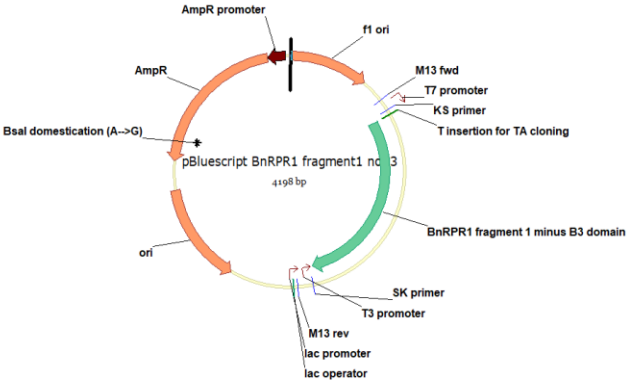

c.

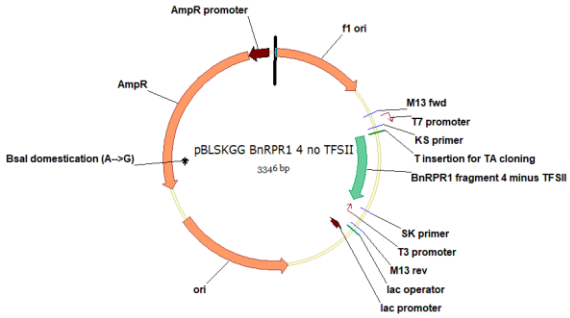

d.

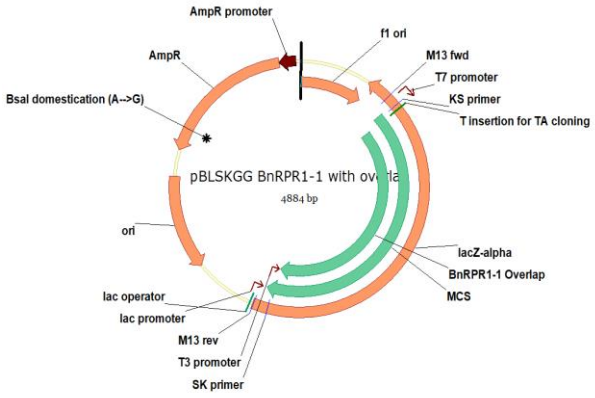

e.

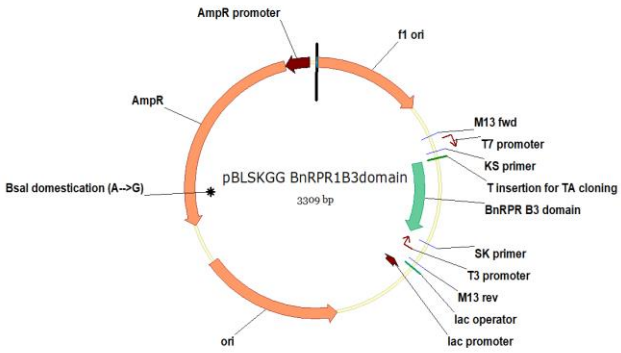

f.

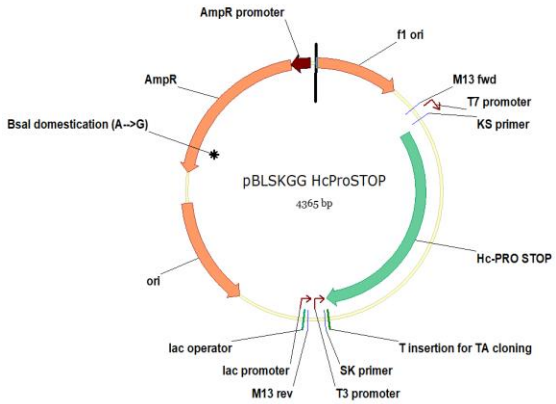

g.

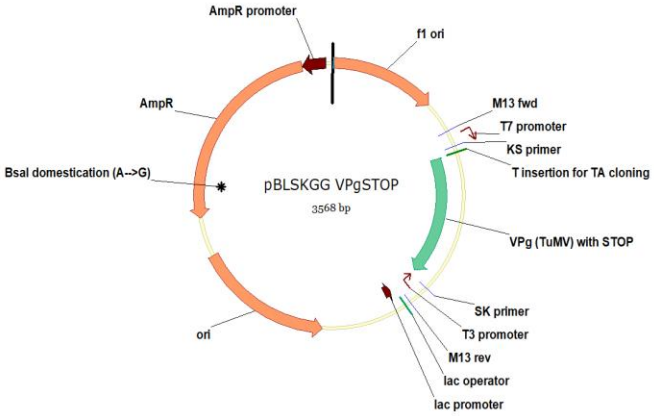

h.

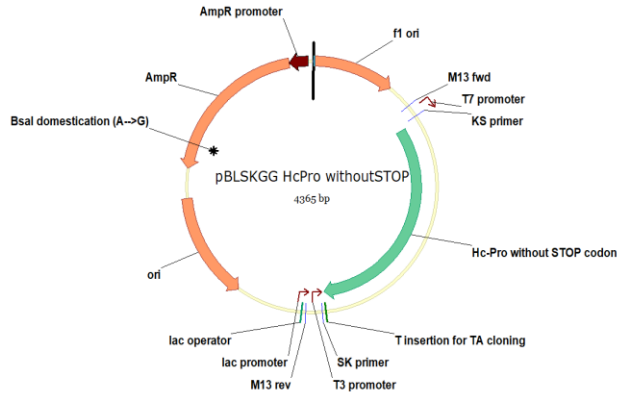

i.

<u>Supplementary figure A</u>. Constructs in pBluescript **a.** PBLSKGG:*Bn*RPR1-4STOP **b**. PBLSKGG:*Bn*RPR2-2STOP **c**. PBLSKGG:*Bn*RPR1-1minusB3 **d.** PBLSKGG:*Bn*RPR1-4minusTFSII **e**. PBLSKGG:5'UTR:*Bn*RPR1-1 **f.** PBLSKGG:*Bn*RPR1B3domain **g**. PBLSKGG:HcProStop **h.** PBLSKGG:VPgSTOP **i**. PBLSKGG:HcProwithoutSTOP

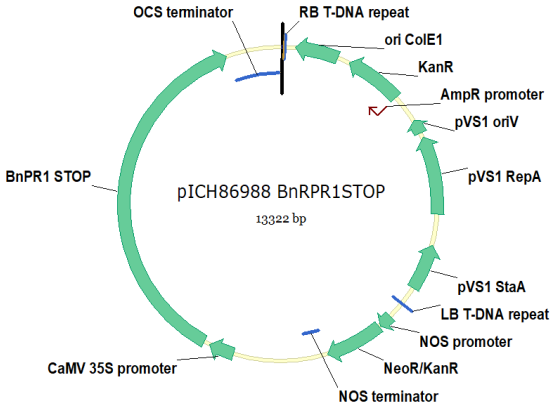
OCS terminator
RB T-DNA repeat
ori ColE1
KanR
AmpR promoter
pVS1 oriV
pVS1 RepA
pVS1 StaA
LB T-DNA repeat
NOS promoter
NeoR/KanR
NOS terminator
CaMV 35S promoter
BnPR1 STOP
pICH86988 BnRPR1STOP
13322 bp

a.

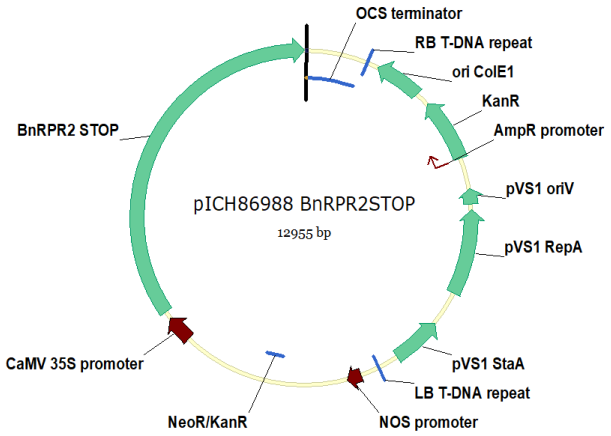
OCS terminator
RB T-DNA repeat
ori ColE1
KanR
AmpR promoter
pVS1 oriV
pVS1 RepA
pVS1 StaA
LB T-DNA repeat
NOS promoter
NeoR/KanR
CaMV 35S promoter
BnRPR2 STOP
pICH86988 BnRPR2STOP
12955 bp

b.

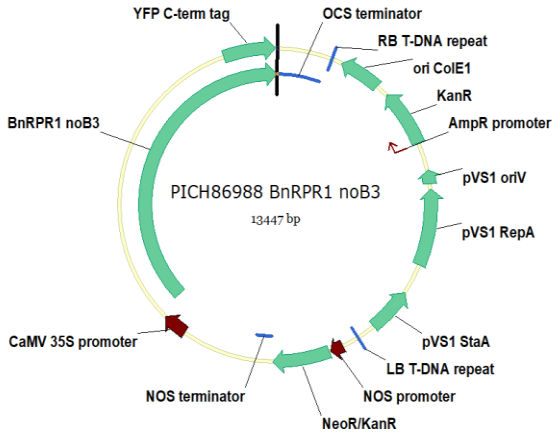
YFP C-term tag
OCS terminator
RB T-DNA repeat
ori ColE1
KanR
AmpR promoter
pVS1 oriV
pVS1 RepA
pVS1 StaA
LB T-DNA repeat
NOS promoter
NeoR/KanR
NOS terminator
CaMV 35S promoter
BnRPR1 noB3
PICH86988 BnRPR1 noB3
13447 bp

c.

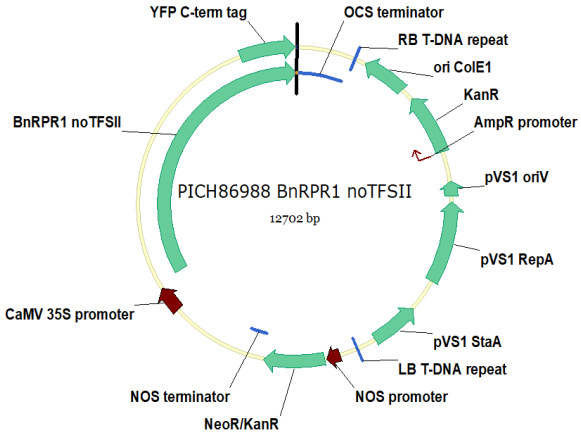
YFP C-term tag
OCS terminator
RB T-DNA repeat
ori ColE1
KanR
AmpR promoter
pVS1 oriV
pVS1 RepA
pVS1 StaA
LB T-DNA repeat
NOS promoter
NeoR/KanR
NOS terminator
CaMV 35S promoter
BnRPR1 noTFSII
PICH86988 BnRPR1 noTFSII
12702 bp

d.

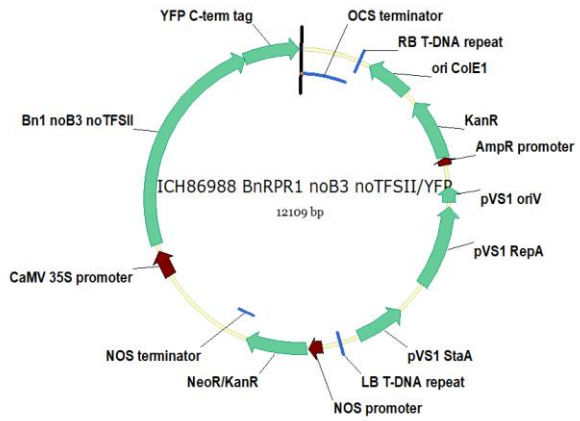
YFP C-term tag
OCS terminator
RB T-DNA repeat
ori ColE1
KanR
AmpR promoter
pVS1 oriV
pVS1 RepA
pVS1 StaA
LB T-DNA repeat
NOS promoter
NeoR/KanR
NOS terminator
CaMV 35S promoter
Bn1 noB3 noTFSII
ICH86988 BnRPR1 noB3 noTFSII/YFP
12109 bp

e.

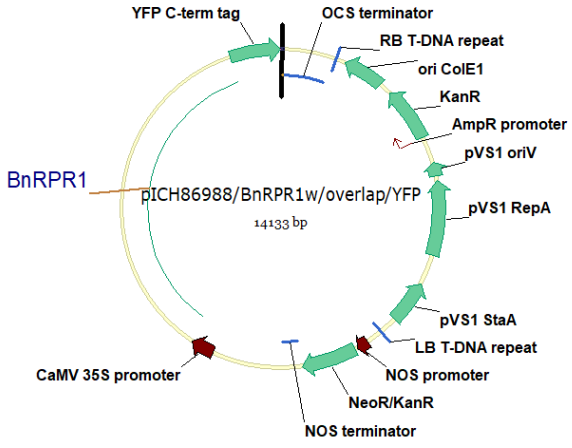
YFP C-term tag
OCS terminator
RB T-DNA repeat
ori ColE1
KanR
AmpR promoter
pVS1 oriV
pVS1 RepA
pVS1 StaA
LB T-DNA repeat
NOS promoter
NeoR/KanR
NOS terminator
CaMV 35S promoter
BnRPR1
pICH86988/BnRPR1w/overlap/YFP
14133 bp

f.

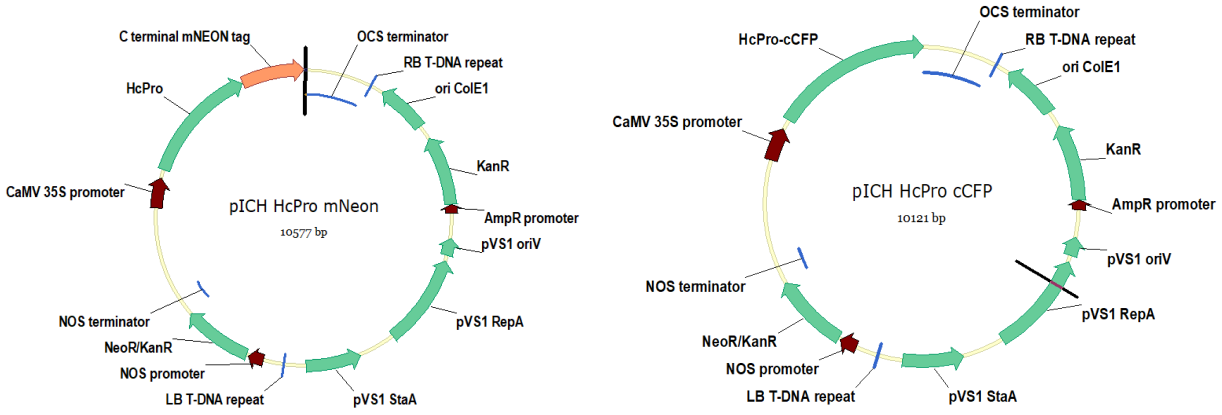

g. **h.**

<u>Supplementary figure B</u>. Constructs in pICH86988 **a.** pICH86988:*Bn*RPR1STOP **b**. pICH86988:*Bn*RPR2STOP **c**. pICH86988:*Bn*RPR1:ΔB3:YFP **d.** pICH86988:*Bn*RPR1:ΔTFSII:YFP **e**. pICH86988: *Bn*RPR1:ΔB3ΔTFSII:YFP **f.** 5'UTR:*Bn*RPR1:YFP **f.** pICH86988:*Bn*RPR1B3domain:YFP **g**. pICH86988:HcPro:mNeon **h.** pICH86988:HcPro:cCFP

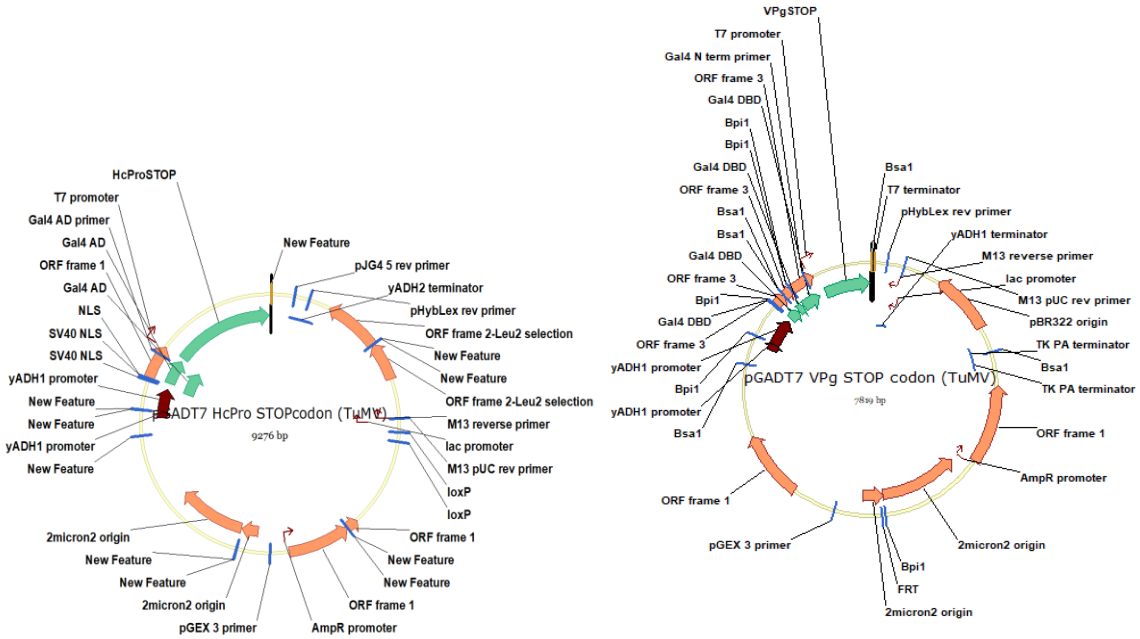

a. **b.**

<u>Supplementary figure C</u>. Constructs in pGADT7 **a.** pGADT7:HcProSTOP **b.** pGADT7:VPgSTOP

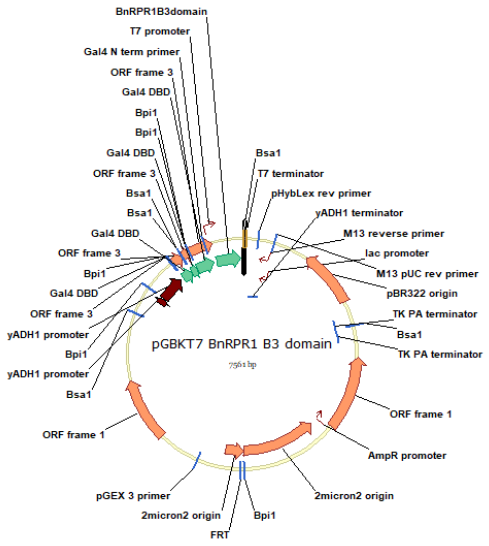

Supplementary figure D. Construct pGBKT7:*Bn*RPR1B3domain

Supplementary table 1. List of primers used in PCR protocols

	forward	reverse
5'UTR:*Bn*RPR1	TTTGGTCTCAAATGTTTCCGGCGAAGAAAATCG	TTTGGTCTCAAAGCCTTCCTGCAAATCAGATCCTTCC
BnRPR1B3domain	TTGGTCTCAAATGTTCGAGAAATGTTTGACAACCAGC	TTTGGTCTCAAAGCTTATTCGCGCCTTCTAAAGCCAATG
HcPro	TTTGGTCTCAAATGAGTGCAGCAGGAGCTAACTTCTG	TTTGGTCTCACGAAGGTCCGACGCGGTAGTGTTTCAAG
HcProSTOP	TTTGGTCTCAAATGAGTGCAGCAGGAGCTAACTTCTG	TTTGGTCTCAAAGCTTATCCGACGCGGTAGTGTTTCAAG
VPgSTOP	TTTGGTCTCAAATGGCGAAAGGTAAGAGGCAAAGAC	TTTGGTCTCAAAGCTTACTCGTGGTCCACTGGGACGAG